

Universal inference meets random projections: a scalable test for log-concavity

Robin Dunn¹, Larry Wasserman^{2,3}, Aaditya Ramdas^{2,3}

¹Novartis Pharmaceuticals Corporation

²Department of Statistics & Data Science, Carnegie Mellon University

³Machine Learning Department, Carnegie Mellon University

November 18, 2021

Abstract

Shape constraints yield flexible middle grounds between fully nonparametric and fully parametric approaches to modeling distributions of data. The specific assumption of log-concavity is motivated by applications across economics, survival modeling, and reliability theory. However, there do not currently exist valid tests for whether the underlying density of given data is log-concave. The recent universal likelihood ratio test provides a valid test. The universal test relies on maximum likelihood estimation (MLE), and efficient methods already exist for finding the log-concave MLE. This yields the first test of log-concavity that is provably valid in finite samples in any dimension, for which we also establish asymptotic consistency results. Empirically, we find that the highest power is obtained by using random projections to convert the d -dimensional testing problem into many one-dimensional problems, leading to a simple procedure that is statistically and computationally efficient.

1 Introduction

Statisticians frequently use density estimation to understand the underlying structure of their data. To perform nonparametric density estimation on a sample, it is common for researchers to incorporate shape constraints (Koenker and Mizera, 2018; Carroll et al., 2011). Log-concavity is one popular choice of shape constraint; a density f is called log-concave if it has the form $f = e^g$ for some concave function g . This class of densities encompasses many common families, such as the normal, uniform (over a compact domain), exponential, logistic, and extreme value densities; see Table 1 of Bagnoli and Bergstrom (2005). Furthermore, specifying that the density is log-concave poses a middle ground between fully nonparametric density estimation and use of a parametric density family. As noted in Cule et al. (2010), log-concave density estimation does not require the choice of a bandwidth, whereas kernel density estimation in d dimensions requires a $d \times d$ bandwidth matrix.

Log-concave densities have multiple appealing properties; An (1997) describes several. For example, log-concave densities are unimodal, they have at most exponentially decaying

tails, i.e., $f(x) = o(\exp(-c\|x\|))$ for some $c > 0$, and all moments of the density exist. Log-concave densities are also closed under convolution, meaning that if X and Y are independent random variables from log-concave densities, then the density of $X + Y$ is log-concave as well. A unimodal density f is strongly unimodal if the convolution of f with any unimodal density g is unimodal. Proposition 2 of An (1997) states that a density f is log-concave if and only if f is strongly unimodal.

In addition, log-concave densities have applications in many domains. Bagnoli and Bergstrom (2005) describe applications of log-concavity across economics, reliability theory, and survival modeling. (The latter two appear to use similar methods in the different domains of engineering and medicine, respectively.) Suppose a survival density function f is defined on (a, b) and has a survival function (or reliability function) $\bar{F}(x) = \int_x^b f(t)dt$. If f is log-concave, then its survival function is log-concave as well. The failure rate associated with f is $r(x) = f(x)/\bar{F}(x) = -\bar{F}'(x)/\bar{F}(x)$. Corollary 2 of Bagnoli and Bergstrom (2005) states that if f is log-concave on (a, b) , then the failure rate $r(x)$ is monotone increasing on (a, b) . Proposition 12 of An (1997) states that if a survival function $\bar{F}(x)$ is log-concave, then for any pair of non-negative numbers x_1, x_2 , the survival function satisfies $\bar{F}(x_1 + x_2) \leq \bar{F}(x_1)\bar{F}(x_2)$. This property is called the new-is-better-than-used property; it implies that the probability that a new unit will survive for time x_1 is greater than or equal to the probability that at time x_2 , an existing unit will survive an additional time x_1 .

Given the favorable properties of log-concave densities and their applications across fields, it is important to be able to test whether the log-concavity assumption holds. Previous researchers have considered this question as well. Cule et al. (2010) develop a permutation test based on simulating from the log-concave MLE and computing the proportion of original and simulated observations in spherical regions. Chen and Samworth (2013) construct an approach similar to the permutation test, using a test statistic based on covariance matrices. Hazelton (2011) develops a kernel bandwidth test, where the test statistic is the smallest kernel bandwidth that produces a log-concave density. Carroll et al. (2011) construct a metric for the necessary amount of modification to the weights of a kernel density estimator to satisfy the shape constraint of log-concavity, and they use the bootstrap to calibrate this metric for testing. While these approaches exhibit reasonable empirical performance in some settings, these tests are not provably valid in finite samples, and they are not asymptotically valid, even with further assumptions. To be clear, none of the aforementioned papers have any proof of validity for their proposed methods. As one exception, An (1997) uses asymptotically normal test statistics to test *implications of* log-concavity (e.g., increasing hazard rate) in the univariate, nonnegative setting, but these are rather restrictive conditions and a general valid test for log-concavity has proved elusive.

As an example, Figure 1 shows the performance of the permutation test of log-concavity from Cule et al. (2010) and a random projection variant of our universal test. Section 3.1 explains the details of the permutation test, and Algorithm 4 explains this universal test. Section 4 provides more extensive simulations. If ϕ_d represents the $N(0, I_d)$ density and $\gamma \in (0, 1)$, then $f(x) = \gamma\phi_d(x) + (1 - \gamma)\phi_d(x - \mu)$ is log-concave only when $\|\mu\| \leq 2$. We simulate the permutation test in this setting for $1 \leq d \leq 5$ and $n = 100$, testing the null hypothesis that the underlying density f^* is log-concave. We set $\mu = (\mu_1, 0, \dots, 0)$, so that $\|\mu\| = \|\mu_1\|$. We use a significance level of $\alpha = 0.10$. Each point represents the proportion

of times we reject H_0 over 200 simulations. Figure 1 shows that the permutation test is valid at $d = 1$ and $d = 2$ and approximately valid at $d = 3$. Alternatively, at $d = 4$ and $d = 5$, this test rejects H_0 at proportions much higher than α , even when the underlying density is log-concave ($\|\mu\| \leq 2$). In contrast, the universal test is valid in all dimensions. Furthermore, this universal test has high power for reasonable $\|\mu\|$ even as we increase d .

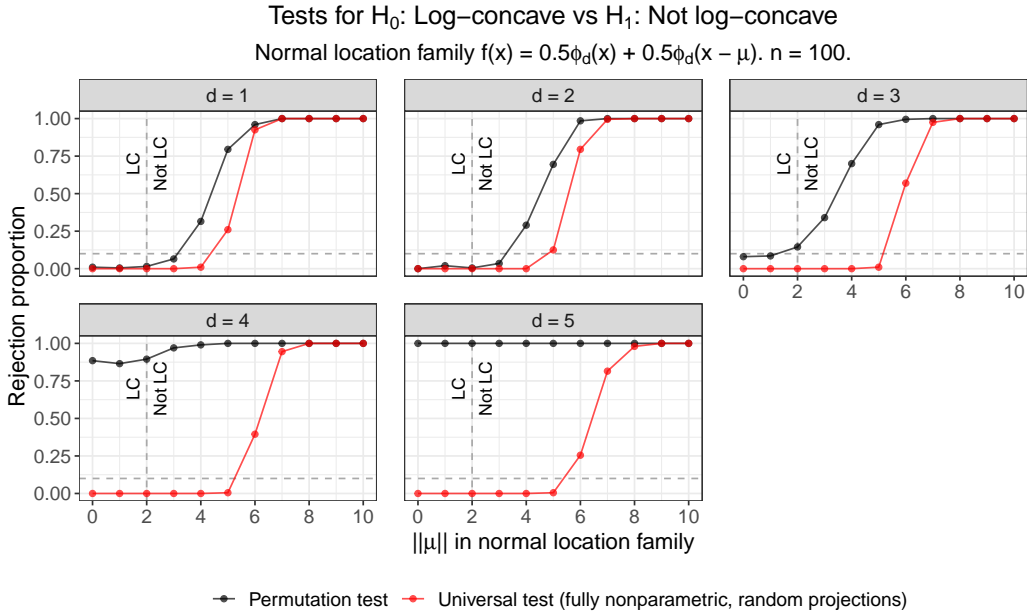


Figure 1: Rejection proportions for tests of $H_0 : f^*$ is log-concave versus $H_1 : f^*$ is not log-concave. The permutation test from Cule et al. (2010) is valid or approximately valid for $d \leq 3$, but it is not valid for $d \geq 4$. Our test that combines random projections and universal inference (Algorithm 4) is provably valid for all n and d while having high power.

To develop a test for log-concavity with validity guarantees, we consider the universal likelihood ratio test (LRT) introduced in Wasserman et al. (2020). This approach provides valid hypothesis tests in any setting in which we can maximize (or upper bound) the null likelihood. Importantly, the validity holds in finite samples and without regularity conditions on the class of models, and thus it holds even in high-dimensional settings without assumptions.

Suppose \mathcal{F}_d is a (potentially nonparametric) class of densities in d dimensions. The universal LRT allows us to test hypotheses of the form $H_0 : f^* \in \mathcal{F}_d$ versus $H_1 : f^* \notin \mathcal{F}_d$. In this paper, \mathcal{F}_d will represent the class of all log-concave densities in d dimensions.

Assume we have n independent and identically distributed (iid) observations Y_1, \dots, Y_n with some true density f^* . To implement the split universal LRT, we randomly partition the indices from 1 to n , denoted as $[n]$, into \mathcal{D}_0 and \mathcal{D}_1 . (Our simulations assume $|\mathcal{D}_0| = |\mathcal{D}_1| = n/2$, but any split proportion is valid.) Using the data indexed by \mathcal{D}_1 , we fit *any* density \hat{f}_1 of our choice, such as a kernel density estimator. The likelihood function evaluated on a density f over the data indexed by \mathcal{D}_0 is denoted $\mathcal{L}_0(f) = \prod_{i \in \mathcal{D}_0} f(Y_i)$. Using the data indexed by \mathcal{D}_0 , we fit $\hat{f}_0 = \arg \max_{f \in \mathcal{F}_d} \mathcal{L}_0(f)$, which is the null maximum likelihood estimator

(MLE). The split LRT statistic is

$$T_n(f) = \mathcal{L}_0(\hat{f}_1) / \mathcal{L}_0(f).$$

The test rejects if $T_n(\hat{f}_0) \geq 1/\alpha$.

Theorem 1 (Wasserman et al. (2020)). *$T_n(\hat{f}_0)$ is an e-value, meaning that it has expectation at most one under the null. Hence, $1/T_n(\hat{f}_0)$ is a valid p-value, and rejecting the null when $T_n(\hat{f}_0) \geq 1/\alpha$ is a valid level- α test. That is, under $H_0 : f^* \in \mathcal{F}_d$,*

$$\mathbb{P}(T_n(\hat{f}_0) \geq 1/\alpha) \leq \alpha.$$

Wasserman et al. (2020) prove Theorem 1, but Appendix A contains a proof for completeness. It is also possible to invert this test, yielding a confidence set for f^* , but for nonparametric classes \mathcal{F}_d , these are not in closed form and are hard to compute numerically, so we do not pursue this direction further. Nevertheless, as long as we are able to construct \hat{f}_0 (or actually simply calculate or upper bound its likelihood), it is possible to perform the nonparametric hypothesis test described in Theorem 1.

Prior to the universal LRT developed by Wasserman et al. (2020), there was no hypothesis test for $H_0 : f^*$ is log-concave versus $H_1 : f^*$ is not log-concave with finite sample validity, or even asymptotic validity. Since it is possible to compute the log-concave MLE on any sample of size $n \geq d + 1$, the universal LRT described above provides a valid test as long as $|\mathcal{D}_0| \geq d + 1$. The randomization in the splitting above can be entirely removed — without affecting the validity guarantee — at the expense of more computation. Wasserman et al. (2020) show that one can repeatedly compute $T_n(\hat{f}_0)$ under independent random splits, and average all the test statistics; since each has expectation at most one under the null, so does their average. It follows that the test based on averaging over multiple splits still has finite sample validity.

Section 2 reviews critical work on the construction and convergence of log-concave MLE densities. Section 3 describes the permutation test from Cule et al. (2010) and proposes several universal tests for log-concavity. The log-concave MLE does suffer from a curse of dimensionality, both computationally and statistically, and so our most important contribution is a scalable method using random projections to reduce the multivariate problem into many univariate testing problems, where the log-concave MLE is easy to compute. (This relies on the fact that if a density is log-concave then every projection is also log-concave.) Section 4 compares these tests through a simulation study. Section 5 explains a theoretical result about the power of the universal LRT for tests of log-concavity. All proofs and several additional simulations are available in the appendices. Code to reproduce all analyses is available at https://github.com/RobinMDunn/Universal_Inference_LogConcave.

2 Finding the Log-concave MLE

Suppose we observe an iid sample $X_1, \dots, X_n \in \mathbb{R}^d$ from a d -dimensional density f^* , where $n \geq d + 1$. Recall that \mathcal{F}_d is the class of all log-concave densities in d dimensions. The log-concave maximum likelihood estimator is $\hat{f}_n = \arg \max_{f \in \mathcal{F}_d} \sum_{i=1}^n \log\{f(X_i)\}$. Theorem 1 of

Cule et al. (2010) states that with probability 1, \widehat{f}_n exists and is unique. Importantly, it is not necessary that $f^* \in \mathcal{F}_d$.

The construction of \widehat{f}_n relies on the concept of a tent function $\bar{h}_y : \mathbb{R}^d \rightarrow \mathbb{R}$. For a given vector $y = (y_1, \dots, y_n) \in \mathbb{R}^n$ and given the sample X_1, \dots, X_n , the tent function \bar{h}_y is the smallest concave function that satisfies $\bar{h}_y(X_i) \geq y_i$ for $i = 1, \dots, n$. Let C_n be the convex hull of the observations X_1, \dots, X_n . Consider the objective function

$$\sigma(y_1, \dots, y_n) = -\frac{1}{n} \sum_{i=1}^n y_i + \int_{C_n} \exp\{\bar{h}_y(x)\} dx.$$

Theorem 2 of Cule et al. (2010) states that σ is a convex function, and it has a unique minimum at the value $y^* \in \mathbb{R}^n$ that satisfies $\log(\widehat{f}_n) = \bar{h}_{y^*}$.

Thus, to find the tent function that defines the log-concave MLE, we need to minimize σ over $y \in \mathbb{R}^n$. σ is not differentiable, but Shor’s algorithm (Shor, 2012) uses a subgradient method to optimize convex, non-differentiable functions. This method is guaranteed to converge, but convergence can be slow. Shor’s r -algorithm involves some computational speed-ups over Shor’s algorithm, and Cule et al. (2010) use this algorithm in their implementation. Shor’s r -algorithm is not guaranteed to converge, but Cule et al. (2010) state that they agree with Kappel and Kuntsevich (2000) that the algorithm is “robust, efficient, and accurate.” The `LogConcDEAD` package for log-concave density estimation in arbitrary dimensions implements this method (Cule et al., 2009).

Alternatively, the `logcondens` package implements an active set approach to solve for the log-concave MLE in one dimension (Dümbgen and Rufibach, 2011). This algorithm is based on solving for a vector that satisfies a set of active constraints and then using the tent function structure to compute the log-concave density associated with that vector. See Section 3.2 of Dümbgen et al. (2007) for more details.

Figure 2 shows the true f^* and log-concave MLE (\widehat{f}_n) densities of several samples from two-component Gaussian mixtures. The underlying density is

$$f^*(x) = 0.5\phi_d(x) + 0.5\phi_d(x - \mu).$$

Again, this density is log-concave if and only if $\|\mu\| \leq 2$. (We develop this example further in Section 4.) In the $n = 5000$ and $d = 1$ setting, we simulate samples $X_1, \dots, X_n \sim f^*$ and compute the log-concave MLE \widehat{f}_n on each random sample. These simulations use both the `LogConcDEAD` and `logcondens` packages to fit \widehat{f}_n . `logcondens` only works in one dimension but is much faster than `LogConcDEAD`. The two packages produce densities with similar appearances. Furthermore, we include values of $n^{-1} \sum_{i=1}^n \log(f^*(x_i))$ on the true density plots and $n^{-1} \sum_{i=1}^n \log(\widehat{f}_n(x_i))$ on the log-concave MLE plots. The log likelihood is approximately the same for the two density estimation methods.

In the first two rows of Figure 2, the true density is log-concave and in this case, we see that $n^{-1} \sum_{i=1}^n \log(\widehat{f}_n(x_i))$ is approximately equal to $n^{-1} \sum_{i=1}^n \log(f^*(x_i))$. When $\|\mu\| = 4$, the underlying density is not log-concave. The log-concave MLE at $\|\mu\| = 4$ and $n = 5000$ seems to have normal tails, but it is nearly uniform in the middle.

Appendix B.1 contains additional plots of the true densities and log-concave MLE densities when $n = 50$ and $d = 1$, $n = 50$ and $d = 2$, and $n = 500$ and $d = 2$. In the smaller

sample $d = 1$ setting, we still observe agreement between `LogConcDEAD` and `logcondens`. When $d = 2$ and the true density is log-concave, the log-concave MLE is closer to the true density at larger n . Alternatively, when $d = 2$ and the true density is not log-concave, the log-concave MLE density again appears to be uniform in the center.

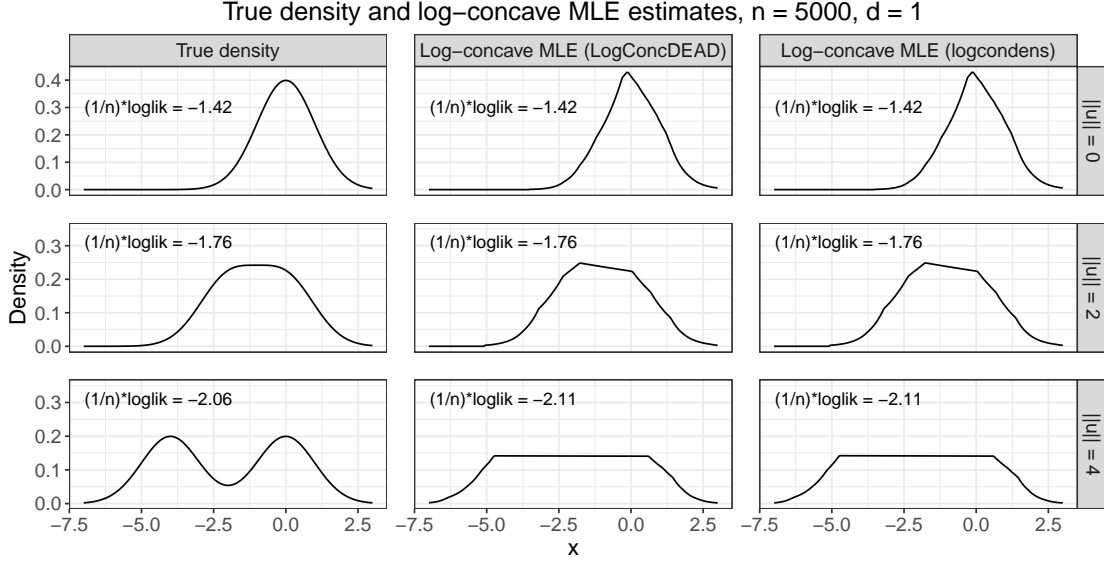


Figure 2: Density plots from fitting log-concave MLE on $n = 5000$ observations. The true density is the Normal mixture $f^*(x) = 0.5\phi_1(x) + 0.5\phi_1(x - \mu)$. In all settings, the `LogConcDEAD` and `logcondens` packages return similar results. In the $\|\mu\| = 0$ and $\|\mu\| = 2$ log-concave settings, the log-concave MLE over 5000 observations is close to the true density. In the $\|\mu\| = 4$ non-log-concave setting, the log-concave densities appear to have normal tails and uniform centers.

Cule et al. (2010) formalize the convergence of \hat{f}_n . Let $D_{\text{KL}}(g||f)$ be the Kullback-Leibler (KL) divergence of g from f . Define $f^{\text{LC}} = \arg \min_{f \in \mathcal{F}_d} D_{\text{KL}}(f^*||f)$ as the KL-projection of f^* onto the set of all log-concave densities. Obviously, if $f^* \in \mathcal{F}_d$, then $f^{\text{LC}} = f^*$. Regardless of whether $f^* \in \mathcal{F}_d$, suppose f^* satisfies the following conditions: $\int_{\mathbb{R}^d} \|x\| f^*(x) dx < \infty$, $\int_{\mathbb{R}^d} f^* \log_+(f^*) < \infty$ (where $\log_+(x) = \max\{\log(x), 0\}$), and the support of f^* contains an open set. By Lemma 1 of Cule and Samworth (2010), there exists some $a_0 > 0$ and $b_0 \in \mathbb{R}$ such that $f^{\text{LC}}(x) \leq \exp(-a_0\|x\| + b_0)$ for any $x \in \mathbb{R}^d$. Theorem 3 of Cule et al. (2010) states that for any $a < a_0$,

$$\int_{\mathbb{R}^d} \exp(a\|x\|) |\hat{f}_n(x) - f^{\text{LC}}(x)| dx \rightarrow 0 \quad \text{almost surely.}$$

This means that the integrated difference between \hat{f}_n and f^{LC} converges to 0 even when we multiply the tails by some exponential weight. Furthermore, Theorem 3 of Cule et al. (2010) states that if f^{LC} is continuous, then

$$\sup_{x \in \mathbb{R}^d} \left\{ \exp(a\|x\|) |\hat{f}_n(x) - f^{\text{LC}}(x)| \right\} \rightarrow 0 \quad \text{almost surely.}$$

In the case where $f^* \in \mathcal{F}_d$, it is possible to describe rates of convergence of the log-concave MLE in terms of the Hellinger distance. The Hellinger distance is given by

$$d_H^2(f, g) = \int_{\mathbb{R}^d} (f^{1/2} - g^{1/2})^2.$$

As stated in Chen et al. (2021) and shown in Kim and Samworth (2016) and Kur et al. (2019), the rate of convergence of \hat{f}_n to f^* in Hellinger distance is

$$\sup_{f^* \in \mathcal{F}_d} \mathbb{E}[d_H^2(\hat{f}_n - f^*)] \leq K_d \cdot \begin{cases} n^{-4/5} & d = 1 \\ n^{-2/(d+1)} \log(n) & d \geq 2 \end{cases},$$

where $K_d > 0$ depends only on d .

3 Tests for Log-concavity

We first describe a permutation test as developed in Cule et al. (2010), and then we propose several universal tests. The latter are guaranteed to control the type I error at level α (theoretically and empirically), while the former is not valid (both theoretically and empirically), as already demonstrated in Figure 1.

3.1 Permutation Test (Cule et al., 2010)

Algorithm 1 Permutation test for $H_0 : f^* \in \mathcal{F}_d$ versus $H_1 : f^* \notin \mathcal{F}_d$

Input: n iid d -dimensional observations Y_1, \dots, Y_n , number of shuffles B , significance level α .

Output: Decision of whether to reject $H_0 : f^* \in \mathcal{F}_d$.

- 1: Fit the log-concave MLE \hat{f}_n on $\mathcal{Y} = \{Y_1, \dots, Y_n\}$.
 - 2: Draw another sample $\mathcal{Y}^* = \{Y_1^*, \dots, Y_n^*\}$ from the log-concave MLE \hat{f}_n .
 - 3: Compute the test statistic $T = \sup_{A \in \mathcal{A}_0} |P_n(A) - P_n^*(A)|$, where \mathcal{A}_0 is the set of all balls centered at a point in $\mathcal{Y} \cup \mathcal{Y}^*$, $P_n(A)$ is the proportion of observations in A out of all observations in \mathcal{Y} , and $P_n^*(A)$ is the proportion of observations in A out of all observations in \mathcal{Y}^* .
 - 4: **for** $b = 1, 2, \dots, B$ **do**
 - 5: ‘Shuffle the stars’ to randomly place n observations from $\mathcal{Y} \cup \mathcal{Y}^*$ into \mathcal{Y}_b .
 - 6: Place the remaining n observations in \mathcal{Y}_b^* .
 - 7: Using these new samples, compute $T_b^* = \sup_{A \in \mathcal{A}_0} |P_{n,b}(A) - P_{n,b}^*(A)|$. $P_{n,b}(A)$ and $P_{n,b}^*(A)$ are defined similarly to $P_n(A)$ and $P_n^*(A)$, using \mathcal{Y}_b and \mathcal{Y}_b^* .
 - 8: Arrange the test statistics $(T_1^*, T_2^*, \dots, T_B^*)$ into the order statistics $(T_{(1)}^*, T_{(2)}^*, \dots, T_{(B)}^*)$.
 - 9: **return** Reject H_0 if $T > T_{(\lceil (B+1)(1-\alpha) \rceil)}^*$.
-

Intuitively, this test assumes that if H_0 is true, the samples \mathcal{Y} and \mathcal{Y}^* will be similar, so T will not be particularly large relative to T_1^*, \dots, T_B^* . Alternatively, if H_0 is false, the samples

\mathcal{Y} and \mathcal{Y}^* will be dissimilar, and the converse will hold. This approach is not guaranteed to control the type I error level. We observe cases both where the permutation test performs well and where the permutation test's false positive rate is much higher than α .

We provide several computational notes on Algorithm 1. Steps 1 and 2 use functions from the `LogConcDEAD` library. To perform step 1, we can use the `ml1cd` function, which estimates the log-concave MLE density from a sample. To perform step 2, we can use the `rlcd` function, which samples from a fitted log-concave density. Where \mathcal{A}_0 is the set of all balls centered at a point in $\mathcal{Y} \cup \mathcal{Y}^*$, $|P_n(A) - P_n^*(A)|$ only takes on finitely many values over $A \in \mathcal{A}_0$. To see this, consider fixing a point at some value $y \in \mathcal{Y} \cup \mathcal{Y}^*$, letting $A_r(y)$ be the sphere of radius r centered at y , and increasing r from 0 to infinity. As $r \rightarrow \infty$, $|P_n(A_r(y)) - P_n^*(A_r(y))|$ only changes when $A_r(y)$ expands to include an additional observation in $\mathcal{Y} \cup \mathcal{Y}^*$. Hence, it is possible to compute $\sup_{A \in \mathcal{A}_0} |P_n(A) - P_n^*(A)|$ by considering all sets A centered at some $y \in \mathcal{Y} \cup \mathcal{Y}^*$ and with radii equal to the distances between the center of A and all other observations. For large n , it may be necessary to approximate the test statistics $T, T_1^*, T_2^*, \dots, T_B^*$ by varying the radius of A across a smaller set of fixed increments. In each of our simulations, we compute the test statistics exactly.

3.2 Universal Tests in d Dimensions

Alternatively, we can use universal approaches to test for log-concavity. Theorem 1 justifies the universal approach for testing whether $f^* \in \mathcal{F}_d$. Recall that the universal LRT provably controls the type I error level in finite samples. To implement the universal test on a single subsample, we partition $[n]$ into \mathcal{D}_0 and \mathcal{D}_1 . Let \hat{f}_0 be the maximum likelihood log-concave density estimate fit on $\{Y_i : i \in \mathcal{D}_0\}$. Let \hat{f}_1 be any density estimate fit on $\{Y_i : i \in \mathcal{D}_1\}$. The universal test rejects H_0 when

$$T_n = \prod_{i \in \mathcal{D}_0} \{\hat{f}_1(Y_i)/\hat{f}_0(Y_i)\} \geq 1/\alpha.$$

The universal test from Theorem 1 holds when T_n is replaced with an average of test statistics, each computed over random partitions of $[n]$. Algorithm 2 explains how to use subsampling to compute a test statistic T_n for the test of $H_0 : f^* \in \mathcal{F}_d$ versus $H_1 : f^* \notin \mathcal{F}_d$. In this case, we reject H_0 when $B^{-1} \sum_{j=1}^B T_{n,j} \geq 1/\alpha$. Note that each test statistic $T_{n,j}$ is nonnegative. In cases where we have sufficient evidence against H_0 , it may be possible to reject H_0 at some iteration $b < B$. That is, for any b such that $1 \leq b < B$, $\sum_{j=b}^B T_{n,j} \geq 0$. If there is a value of $b < B$ such that $B^{-1} \sum_{j=1}^b T_{n,j} \geq 1/\alpha$, then it is guaranteed that $T_n = B^{-1} \sum_{j=1}^B T_{n,j} \geq 1/\alpha$. Algorithms 2–4 incorporate this fact by rejecting early if we have sufficient evidence against H_0 .

Algorithm 2 For $H_0 : f^* \in \mathcal{F}_d$ versus $H_1 : f^* \notin \mathcal{F}_d$, compute the subsampling test statistic or run the test.

Input: n iid d -dimensional observations Y_1, \dots, Y_n with density f^* ,
number of subsamples B , any density estimation approach.

Output: The subsampling test statistic T_n or the test result.

- 1: **for** $b = 1, 2, \dots, B$ **do**
 - 2: Randomly partition $[n]$ into $\mathcal{D}_{0,b}$ and $\mathcal{D}_{1,b}$ such that $|\mathcal{D}_{0,b}| = |\mathcal{D}_{1,b}| = n/2$.
 - 3: Where $\mathcal{L}_{0,b}(f) = \prod_{i \in \mathcal{D}_{0,b}} f(Y_i)$, compute $\hat{f}_{0,b} = \arg \max_{f \in \mathcal{F}_d} \mathcal{L}_{0,b}(f)$.
 - 4: Fit a density $\hat{f}_{1,b}$ on $\{Y_i : i \in \mathcal{D}_{1,b}\}$, using the input density estimation approach.
 - 5: Compute $T_{n,b} = \mathcal{L}_{0,b}(\hat{f}_{1,b}) / \mathcal{L}_{0,b}(\hat{f}_{0,b})$.
 - 6: **if** $B^{-1} \sum_{j=1}^b T_{n,j} \geq 1/\alpha$ **then return** rejection of hypothesis.
 - 7: **return** the subsampling test statistic $T_n = B^{-1} \sum_{j=1}^B T_{n,j}$.
-

Both `logcondens` ($d = 1$) and `LogConcDEAD` ($d \geq 1$) provide functions to compute the log-concave MLE \hat{f}_0 . We have flexibility in the choice of \hat{f}_1 , which can be any density. We explore several choices of \hat{f}_1 .

Full Oracle The full oracle approach uses the d -dimensional true density f^* in the numerator. In Algorithm 2, the input density estimation approach is to set $\hat{f}_{1,b} = f^*$. This method is a helpful theoretical comparison, since it avoids the depletion in power that occurs when $\hat{f}_{1,b}$ does not approximate f^* well. We would expect the power of this approach to be greater than or equal to the power of any approach that estimates a numerator density on $\{Y_i : i \in \mathcal{D}_{1,b}\}$.

Partial Oracle The partial oracle approach uses a d -dimensional parametric MLE density estimate in the numerator. Suppose we know (or we guess) that the true density is parameterized by some unknown real-valued vector $\theta^* \in \mathbb{R}^p$ such that $f^* = f_{\theta^*}$. Let $\mathcal{L}_{1,b}(f_\theta) = \prod_{i \in \mathcal{D}_{1,b}} f_\theta(Y_i)$. In Algorithm 2, the input density estimation approach is to set $\hat{f}_{1,b} = f_{\hat{\theta}_{1,b}}$, where $\hat{\theta}_{1,b} = \arg \max_{\theta \in \mathbb{R}^p} \mathcal{L}_{1,b}(f_\theta)$. If the true density is from the parametric family $(f_\theta : \theta \in \mathbb{R}^p)$, we would expect this method to have good power relative to other density estimation methods.

Fully Nonparametric The fully nonparametric method uses a d -dimensional kernel density estimate (KDE) in the numerator. In Algorithm 2, the input density estimation approach is to set $\hat{f}_{1,b}$ to the kernel density estimate computed on $\mathcal{D}_{1,b}$. Kernel density estimation involves the choice of a bandwidth. The `ks` package (Duong, 2021) in `R` can fit multidimensional KDEs and has several bandwidth computation procedures. These options include a plug-in bandwidth (Wand and Jones, 1994; Duong and Hazelton, 2003; Chacón and Duong, 2010), a least squares cross-validated bandwidth (Bowman, 1984; Rudemo, 1982), and a smoothed cross-validation bandwidth (Jones et al., 1991; Duong and Hazelton, 2005). In the parametric density case, we would expect the fully nonparametric method to have lower power than

the full oracle method and the partial oracle method. If we do not want to make assumptions about the true density, this may be a good choice.

3.3 Universal Tests with Dimension Reduction

Suppose we write each random variable $Y \in \mathbb{R}^d$ as $Y = (Y^{(1)}, \dots, Y^{(d)})$. As noted in An (1997), if the density of Y is log-concave, then the marginal densities of $Y^{(1)}, \dots, Y^{(d)}$ are all log-concave. In the converse direction, if marginal densities of $Y^{(1)}, \dots, Y^{(d)}$ are all log-concave and $Y^{(1)}, \dots, Y^{(d)}$ are all independent, then the density of Y is log-concave. Proposition 1 of Cule et al. (2010) uses a result from Prékopa (1973) to deduce a more general result. We restate Proposition 1 in Theorem 2.

Theorem 2 (Proposition 1 of Cule et al. (2010)). *Suppose $Y \in \mathbb{R}^d$ is a random variable from a distribution having density f^* with respect to Lebesgue measure. Where V is a subspace of \mathbb{R}^d , we denote the orthogonal projection of y onto V as $P_V(y)$.*

- (a) *Suppose V is any subspace of \mathbb{R}^d . If f^* is log-concave, then the marginal density of $P_V(Y)$ is log-concave and the conditional density $f_{Y|P_V(Y)}^*(\cdot | t)$ of Y given $P_V(Y) = t$ is log-concave for each t .*
- (b) *Suppose that for every $(d - 1)$ -dimensional subspace V and for each $t \in \mathbb{R}$, the conditional density $f_{Y|P_V(Y)}^*(\cdot | t)$ of Y given $P_V(Y) = t$ is log-concave. Then f^* is log-concave.*

When considering how to test for log-concavity, An (1997) notes that univariate tests for log-concavity could be used in the multivariate setting. For our purposes, we use the Theorem 2(a) implication that if f^* is log-concave, then the one-dimensional projections of f^* are also log-concave. We develop new universal tests on these one-dimensional projections.

To reduce the data to one dimension, we take one of two approaches.

3.3.1 Dimension Reduction Approach 1: Axis-aligned Projections

We can represent any d -dimensional observation Y_i as $Y_i = (Y_i^{(1)}, Y_i^{(2)}, \dots, Y_i^{(d)})$. Algorithm 3 describes an approach that computes a test statistic for each of the d dimensions.

Algorithm 3 For $H_0 : f^* \in \mathcal{F}_d$ versus $H_1 : f^* \notin \mathcal{F}_d$, compute the axis-aligned projection test statistics or run the test.

Input: n iid d -dimensional observations Y_1, \dots, Y_n , number of subsamples B .

Output: d test statistics $T_n^{(k)}$, $k = 1, \dots, d$, or the test result.

- 1: **for** $k = 1, 2, \dots, d$ **do**
 - 2: **for** $b = 1, 2, \dots, B$ **do**
 - 3: Randomly partition $[n]$ into $\mathcal{D}_{0,b}$ and $\mathcal{D}_{1,b}$ such that $|\mathcal{D}_{0,b}| = |\mathcal{D}_{1,b}| = n/2$.
 - 4: Estimate a one-dimensional density $\hat{f}_{1,b}$ on $\{Y_i^{(k)} : i \in \mathcal{D}_{1,b}\}$.
 - 5: Estimate the log-concave MLE $\hat{f}_{0,b}$ on $\{Y_i^{(k)} : i \in \mathcal{D}_{0,b}\}$.
 - 6: **if** $B^{-1} \sum_{j=1}^b \prod_{i \in \mathcal{D}_{0,j}} \{\hat{f}_{1,j}(Y_i^{(k)}) / \hat{f}_{0,j}(Y_i^{(k)})\} \geq d/\alpha$ **then stop**, reject null.
 - 7: Compute the test statistic $T_n^{(k)} = B^{-1} \sum_{b=1}^B \prod_{i \in \mathcal{D}_{0,b}} \{\hat{f}_{1,b}(Y_i^{(k)}) / \hat{f}_{0,b}(Y_i^{(k)})\}$
 - 8: **return** the test statistics $T_n^{(k)}$, $k = 1, \dots, d$.
-

We reject $H_0 : f^* \in \mathcal{F}_d$ if at least one of the d test statistics $T_n^{(1)}, \dots, T_n^{(d)}$ exceeds d/α . Instead of checking this condition at the very end of the algorithm, we check this along the way, and we stop early to save computation if it happens (line 6). This rejection rule has valid type I error control because under H_0 ,

$$\mathbb{P}(T_n^{(1)} \geq d/\alpha \cup T_n^{(2)} \geq d/\alpha \cup \dots \cup T_n^{(d)} \geq d/\alpha) \leq \sum_{k=1}^d \mathbb{P}(T_n^{(k)} \geq d/\alpha) \leq d(\alpha/d) = \alpha.$$

If we do not simply want an accept-reject decision but would instead like a real-valued measure of evidence, then it is easy to check that $p_n := d \min_{k \in [d]} 1/T_n^{(k)}$ is a valid p-value. Indeed the above equation can be rewritten as the statement $\mathbb{P}(p_n \leq \alpha) \leq \alpha$, meaning that under the null, the distribution of p_n is stochastically larger than uniform.

Above, we fit some one-dimensional density $\hat{f}_{1,b}$ on $\{Y_i^{(k)} : i \in \mathcal{D}_{1,b}\}$. We consider two density estimation methods; the same applies to the next subsection.

Density Estimation Method 1: Partial Oracle This approach uses parametric knowledge about the underlying density. The numerator $\hat{f}_{1,b}$ is the parametric MLE fit on $\mathcal{D}_{1,b}$.

Density Estimation Method 2: Fully Nonparametric This approach does not use any prior knowledge about the underlying density. Instead, we use kernel density estimation (e.g., `ks` package with plug-in bandwidth) to fit $\hat{f}_{1,b}$.

Thus, for the universal LRTs with dimension reduction, we consider four total combinations of two dimension reduction approaches and two density estimation methods.

3.3.2 Dimension Reduction Approach 2: Random Projections

We can also construct one-dimensional densities by projecting the data onto a vector drawn uniformly from the unit sphere. Algorithm 4 shows how to compute the random projection test statistic T_n . As discussed in Section 3.2, Theorem 1 justifies the validity of this approach.

In short, each $T_{n,j}$ is an e-value, meaning that it has expectation at most one under the null, and thus so does their average.

Algorithm 4 For $H_0 : f^* \in \mathcal{F}_d$ versus $H_1 : f^* \notin \mathcal{F}_d$, compute the random projection test statistic or run the test.

Input: n iid d -dimensional observations Y_1, \dots, Y_n , number of subsamples B , number of random projections n_{proj} .

Output: The random projection test statistic T_n or the test result.

- 1: **for** $k = 1, 2, \dots, n_{\text{proj}}$ **do**
 - 2: Draw a vector V uniformly from the d -dimensional unit sphere. To obtain V , draw $X \sim N(0, I_d)$ and set $V = X/\|X\|$.
 - 3: Project each Y observation onto V . The projection of Y_i is $P_V(Y_i) = Y_i^T V$.
 - 4: **for** $b = 1, 2, \dots, B$ **do**
 - 5: Randomly partition $[n]$ into $\mathcal{D}_{0,b}$ and $\mathcal{D}_{1,b}$ such that $|\mathcal{D}_{0,b}| = |\mathcal{D}_{1,b}| = n/2$.
 - 6: Estimate a one-dimensional density $\hat{f}_{1,b}$ on $\{P_V(Y_i) : i \in \mathcal{D}_{1,b}\}$.
 - 7: Estimate the log-concave MLE $\hat{f}_{0,b}$ on $\{P_V(Y_i) : i \in \mathcal{D}_{0,b}\}$.
 - 8: Compute the test statistic $T_{n,k} = B^{-1} \sum_{b=1}^B \prod_{i \in \mathcal{D}_{0,b}} \{\hat{f}_{1,b}(P_V(Y_i)) / \hat{f}_{0,b}(P_V(Y_i))\}$.
 - 9: **if** $n_{\text{proj}}^{-1} \sum_{j=1}^k T_{n,j} \geq 1/\alpha$ **then stop**, reject null.
 - 10: **return** the random projection test statistic $T_n = n_{\text{proj}}^{-1} \sum_{j=1}^{n_{\text{proj}}} T_{n,j}$.
-

We expect random projections (with averaging) to work better when the deviations from log-concavity are “dense,” meaning there is a small amount of evidence to be found scattered in different directions. In contrast, the axis-aligned projections (with Bonferroni) presented earlier are expected to work better when there is a strong signal along one or a few dimensions, with most dimensions carrying no evidence (meaning that the density is indeed log-concave along most axes).

4 Example: Testing Log-concavity of Normal Mixture

We test the permutation approach and the universal approaches on a normal mixture distribution, which is log-concave only at certain parameter values. Naturally, when testing or fitting log-concave distributions in practice, one would eschew all parametric assumptions, so the restriction to normal mixtures is simply for a nice simulation example. See Appendix C for another example that applies the universal and permutation tests on the Beta density.

Suppose ϕ_d is the $N(0, I_d)$ density. Cule et al. (2010) note a result that we state in Fact 1.

Fact 1. For $\gamma \in (0, 1)$, the normal location mixture $f(x) = \gamma\phi_d(x) + (1 - \gamma)\phi_d(x - \mu)$ is log-concave only when $\|\mu\| \leq 2$.

We prove this fact in Appendix A for completeness. As some intuition for the one-dimensional case, log-concave densities are unimodal and have at most exponential tails. A one-dimensional mixture of two Gaussians with means μ_1, μ_2 and standard deviations σ_1, σ_2 is unimodal if $|\mu_2 - \mu_1| \leq 2 \min\{\sigma_1, \sigma_2\}$ (Sitek, 2016).

Cule et al. (2010) use the permutation test to test $H_0 : f^* \in \mathcal{F}_d$ versus $H_1 : f^* \notin \mathcal{F}_d$ in this setting. We explore the power and validity of both the permutation test and the universal tests over varying $\|\mu\|$ and dimensions $d \in \{1, 2, 3, 4\}$. We use $\gamma = 0.5$ in all analyses.

4.1 Full Oracle (in d dimensions) has Inadequate Power

We compare the permutation test and the full oracle universal test. Figure 1 showed that the permutation test is not valid in this setting for $d \geq 4$, $n = 100$, and $B = 99$. In Appendix B.2, we show that the rejection proportion is similar if we increase B to $B \in \{100, 200, 300, 400, 500\}$. In addition, we show that if we increase n to 250, the rejection proportion is still much higher than 0.10 for $\|\mu\| \leq 2$ at $d = 4$ and $d = 5$. In the same appendix, we also show that the discrete nature of the test statistic is not the reason for the test's conservativeness (e.g., $d = 1$) or anticonservativeness (e.g., $d = 5$).

To compare the permutation test to the full oracle universal test, we again set $\mu = (\mu_1, 0, \dots, 0)$. Figure 3 shows the power for $d \in \{1, 2, 3, 4\}$ on $n = 100$ observations. For the universal test, we subsample $B = 100$ times. Each point is the rejection proportion over 200 simulations. For some $\|\mu\|$ values in the $d = 1$ case, the full oracle test has higher power than the permutation test. For most $(d, \|\mu\|)$ combinations, though, the full oracle test has lower power than the permutation test. Unlike the permutation test, though, the universal test is provably valid for all d .

In Figure 3, we see that as d increases, we need larger $\|\mu\|$ for the universal test to have power. More specifically, $\|\mu\|$ needs to grow exponentially with d to maintain a certain level of power. (See Figure 13 in Appendix B.3.)

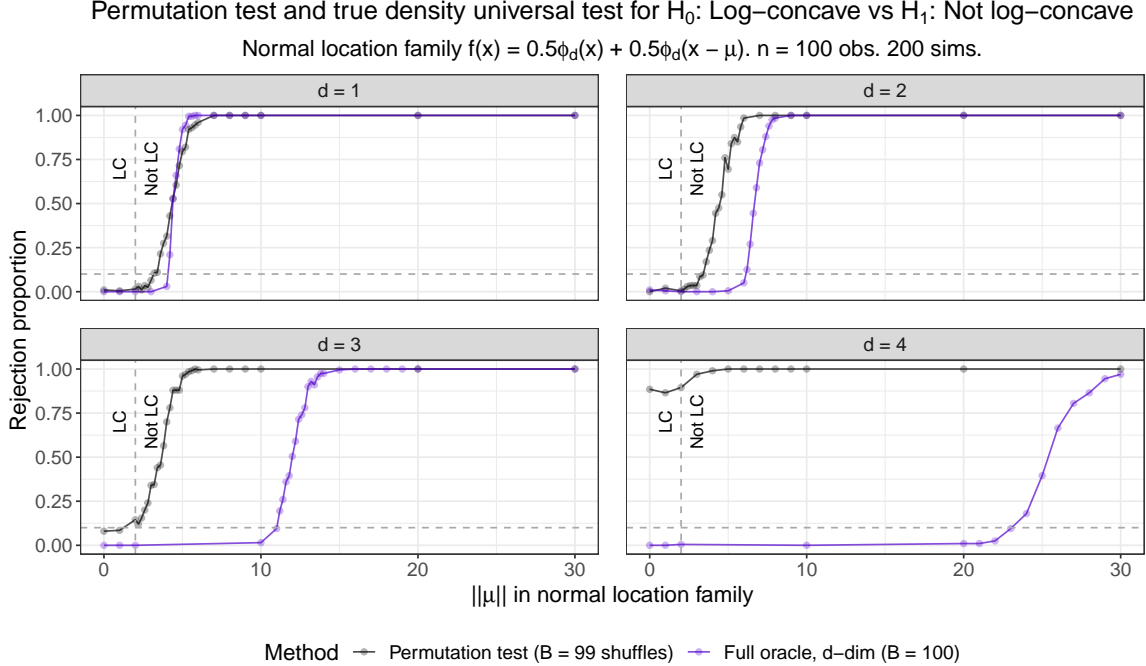


Figure 3: Rejection proportions for tests of $H_0 : f^*$ is log-concave versus $H_1 : f^*$ is not log-concave. When $d = 1$, the permutation test and the full oracle universal test have similar power. The universal approach that uses the true density in the numerator remains valid in higher dimensions, but it has low power for moderate $\|\mu\|$ when $d \geq 3$.

4.2 Superior Performance of Dimension Reduction Approaches

We have seen that the full oracle universal LRT requires $\|\mu\|$ to grow exponentially to maintain power as d increases. We turn to the dimension reduction universal LRT approaches, and we find that they produce higher power for smaller $\|\mu\|$ values.

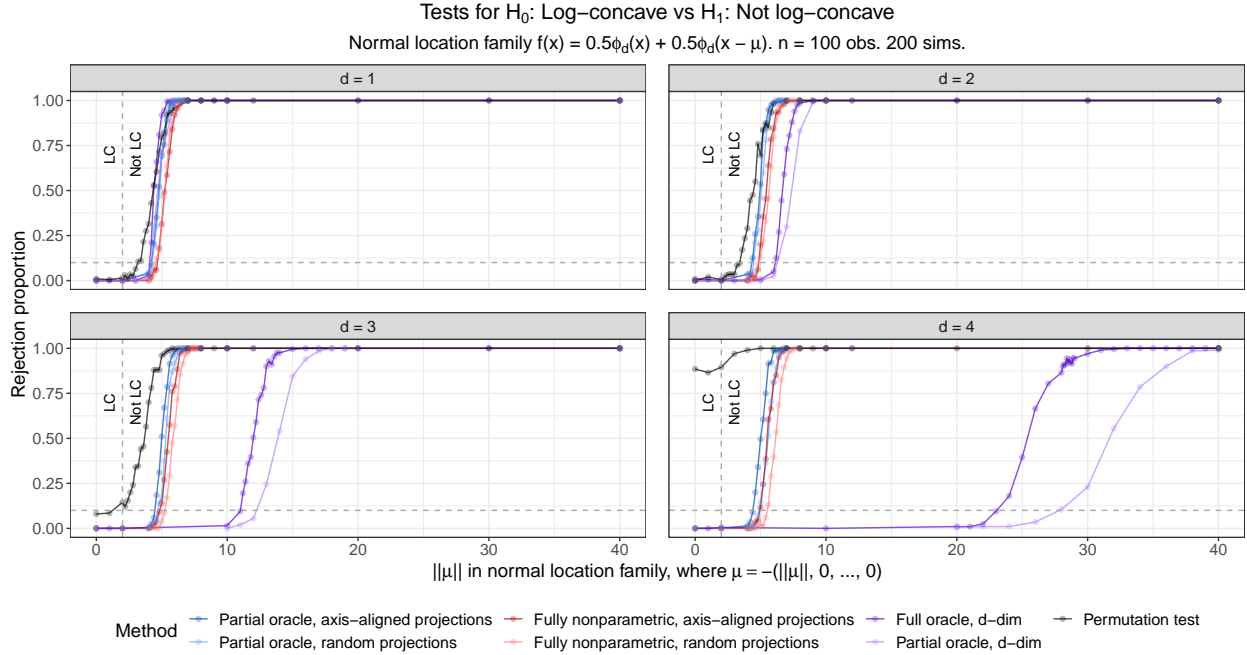
We implement all four combinations of the two dimension reduction approaches (axis-aligned and random projections) and two density estimation methods (partial oracle and fully nonparametric). We compare them to three d -dimensional approaches: the permutation test, the full oracle test, and the partial oracle test. The full oracle d -dimensional approach uses the split LRT with the true density in the numerator and the d -dimensional log-concave MLE in the denominator. The partial oracle d -dimensional approach uses the split LRT with a two component Gaussian mixture in the numerator and the d -dimensional log-concave MLE in the denominator. We fit the Gaussian mixture using the EM algorithm, as implemented in the `mclust` package (Scrucca et al., 2016).

Figures 4 and 5 compare the four dimension reduction approaches and the d -dimensional approaches. The six universal approaches subsample at $B = 100$. The random projection approaches set $n_{\text{proj}} = 100$. The permutation test uses $B = 99$ permutations to determine the significance level of the original test statistic. Both figures use the normal location model $f^*(x) = 0.5\phi_d(x) + 0.5\phi_d(x - \mu)$ as the underlying model. However, Figure 4 uses $\mu = -(\|\mu\|, 0, \dots, 0)$, while Figure 5 uses $\mu = -(\|\mu\|d^{-1/2}, \|\mu\|d^{-1/2}, \dots, \|\mu\|d^{-1/2})$. The axis-aligned projection method has higher power in the first setting, but the other methods

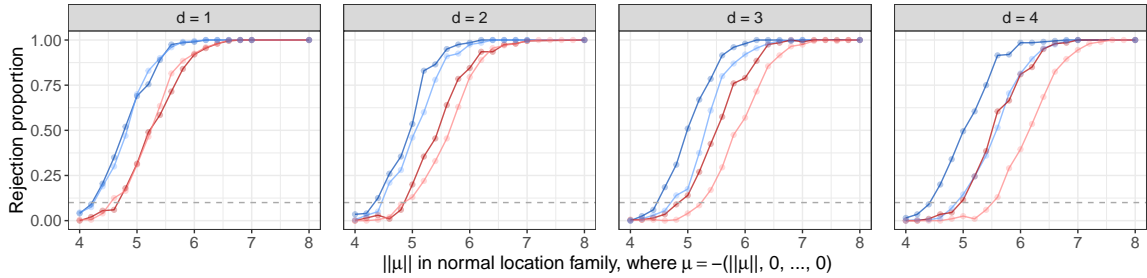
do not have differences in power between the two settings.

Figures 4a and 5a compare all seven methods. There are several key takeaways. The universal approaches that fit one-dimensional densities (axis-aligned projections and random projections) have higher power than the universal approaches that fit d -dimensional densities. (When $d = 1$, the “Partial oracle, axis-aligned projections,” “Partial oracle, d -dim,” and “Partial oracle, random projections” approaches are the same, except that the final method uses Bn_{proj} subsamples rather than B subsamples.) The permutation test is not always valid, especially for $d \geq 4$.

To compare the four universal approaches that fit one-dimensional densities, we consider Figures 4b and 5b, which zoom in on a smaller range of $\|\mu\|$ values for those four methods. In both Figure 4b and 5b, for a given dimension reduction approach (axis-aligned projections or random projections), the partial oracle approach has slightly higher power than the fully nonparametric approach. (That is, the dark blue curve has higher power than the dark red curve, and the light blue curve has higher power than the light red curve.) For a given density estimation approach, the dimension reduction approach with higher power changes based on the setting. When $\mu = -(\|\mu\|, 0, \dots, 0)$ (Figure 4b), the axis-aligned projection approach has higher power than the random projections approach. (That is, dark blue has higher power than light blue, and dark red has higher power than light red.) This makes sense because a single dimension contains all of the signal. When $\mu = -(\|\mu\|d^{-1/2}, \|\mu\|d^{-1/2}, \dots, \|\mu\|d^{-1/2})$ (Figure 5b), the random projections approach has higher power than the axis-aligned projection approach. (That is, light blue has higher power than dark blue, and light red has higher power than dark red.) This makes sense because all directions have some evidence against H_0 , and there exist linear combinations of the coordinates that have higher power than any individual dimension.

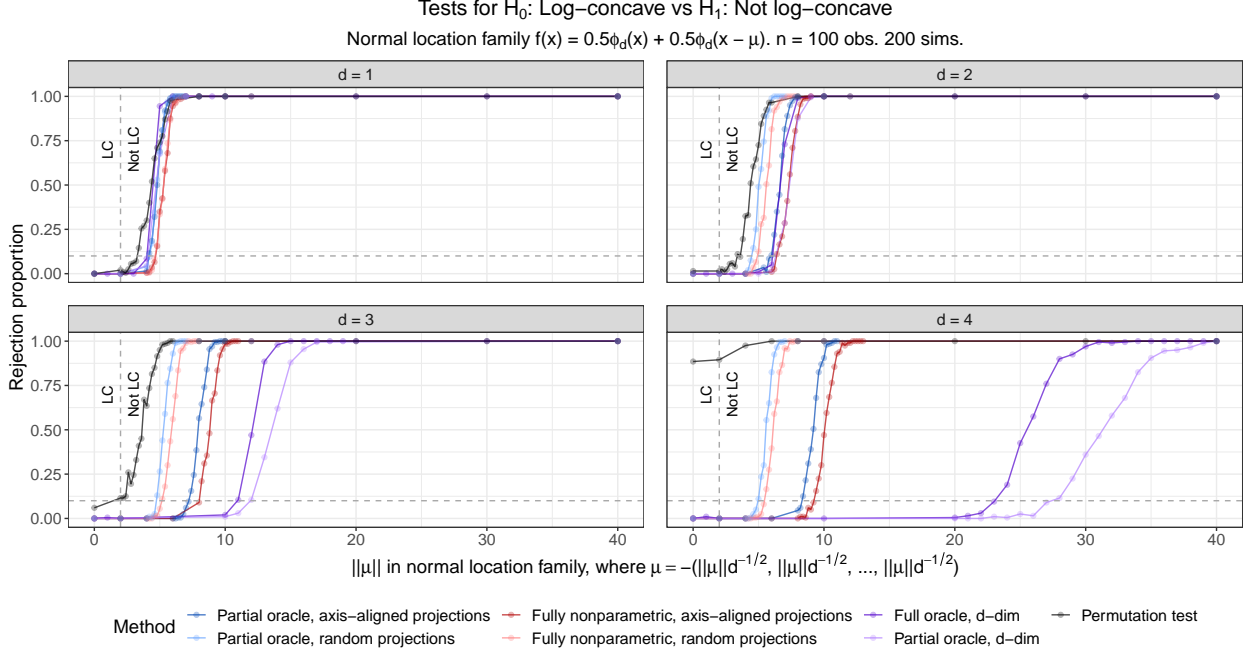


(a) The projection-based universal tests decrease the gap in power between the permutation test and the d -dimensional universal tests for $d \geq 2$. The power of the projection tests only exhibits a moderate curse of dimensionality.

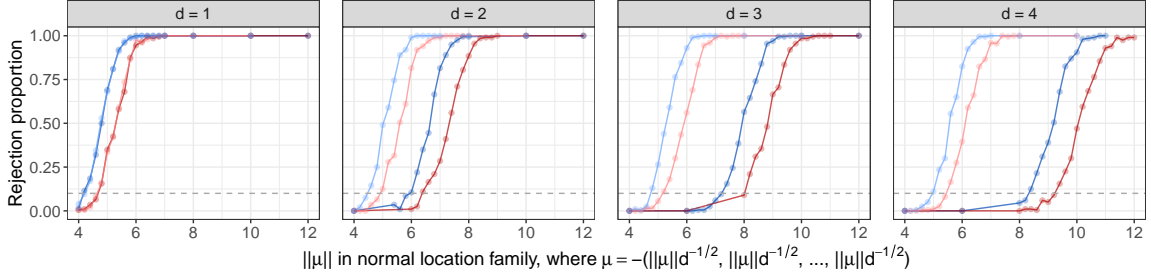


(b) Partial oracle numerators have higher power than fully nonparametric numerators. When all signal against H_0 is in the first component of μ , the axis-aligned projection tests have higher power than the random projection tests within each choice of numerator.

Figure 4: Power of tests of $H_0 : f^*$ is log-concave versus $H_1 : f^*$ is not log-concave. μ vector for second component is $\mu = -(\|\mu\|, 0, \dots, 0)$.



(a) In this second choice of μ structure, the projection-based universal tests also decrease the gap in power between the permutation test and the d -dimensional universal tests for $d \geq 2$. The power of the projection tests only exhibits a moderate curse of dimensionality.



(b) When signal against H_0 is equally distributed across the components of μ , the random projection tests have higher power than the axis-aligned projection tests.

Figure 5: Power of tests of $H_0 : f^*$ is log-concave versus $H_1 : f^*$ is not log-concave. μ vector for second component is $\mu = -(\|\mu\|d^{-1/2}, \|\mu\|d^{-1/2}, \dots, \|\mu\|d^{-1/2})$.

4.3 Time Benchmarking

Table 1 displays the average run times of the seven methods that we consider. Each cell corresponds to an average (in seconds) over 10 simulations at $(\|\mu\| = 0, \|\mu\| = 5, \|\mu\| = 10)$. Except for the restriction on $\|\mu\|$, these simulations use the same parameters as Figure 4. We arrange the methods in rough order from longest to shortest run times in $d = 1$. The random projection methods have some of the longest run times at $\|\mu\| = 0$. If the random projection methods do not have sufficient evidence to reject H_0 early, they will construct Bn_{proj} test statistics. Each of those Bn_{proj} test statistics requires fitting a one-dimensional log-concave MLE and estimating a partial oracle or fully nonparametric numerator density.

The permutation test is faster than the random projection tests in the $\|\mu\| = 0$ setting, but it does not stop early for larger $\|\mu\|$. This method can be prohibitively computationally expensive for large n or d . The axis projection and d -dimensional universal approaches have similar run times for $d \leq 2$. (In fact, for $d = 1$ the partial oracle axis projection and partial oracle d -dimensional methods are the same.) The axis projection methods compute a maximum of Bd test statistics, and the d -dimensional methods compute a maximum of B test statistics. Since the d -dimensional universal approaches repeatedly fit d -dimensional log-concave densities, they are the most computationally expensive approaches for large d .

Method	$d = 1$	$d = 2$	$d = 3$	$d = 4$
Partial oracle, random projections	(180, 99, 0.97)	(180, 77, 1.2)	(160, 190, 3.2)	(120, 110, 4.5)
Fully NP, random projections	(81, 49, 0.46)	(80, 69, 0.89)	(77, 71, 1.9)	(78, 74, 2.1)
Permutation test	(44, 45, 44)	(45, 46, 45)	(47, 47, 47)	(53, 55, 50)
Partial oracle, axis projections	(9.4, 4.5, 0.088)	(18, 7.2, 0.21)	(32, 20, 0.29)	(33, 15, 0.34)
Fully NP, axis projections	(6.5, 4.2, 0.056)	(12, 9.7, 0.12)	(17, 12, 0.18)	(23, 20, 0.23)
Partial oracle, d-dim	(6, 2.5, 0.072)	(18, 18, 0.63)	(62, 65, 65)	(270, 410, 400)
Full oracle, d-dim	(5.2, 1.9, 0.058)	(17, 18, 0.18)	(63, 64, 66)	(270, 290, 290)

Table 1: Average run time (in seconds) of log-concave tests at ($\|\mu\| = 0, \|\mu\| = 5, \|\mu\| = 10$), using the same parameters as Figure 4. The universal methods run faster when there is more evidence against H_0 , which allows for early rejection. It is faster to compute log-concave MLEs in one dimension (e.g., projection methods) than in general d dimensions.

5 Theoretical Power of Log-concave Universal Tests

Through simulations, we have shown that the universal LRTs can have high power in tests of $H_0 : f^* \in \mathcal{F}_d$ versus $H_1 : f^* \notin \mathcal{F}_d$. We now prove a theoretical result that provides conditions under which the power of the universal tests converges to 1. First, we review or introduce some notation. Let $\hat{f}_{1,n}$ be an estimate of f^* , fit on $\mathcal{D}_{1,n}$. Let $\hat{f}_{0,n} = \arg \max_{f \in \mathcal{F}_d} \sum_{i \in \mathcal{D}_{0,n}} \log(f(Y_i))$. In words, $\hat{f}_{0,n}$ is the log-concave MLE fit on $\{Y_i : i \in \mathcal{D}_{0,n}\}$.

The universal test statistic is

$$T_n = \prod_{i \in \mathcal{D}_{0,n}} \frac{\hat{f}_{1,n}(Y_i)}{\hat{f}_{0,n}(Y_i)}.$$

We reject H_0 if $T_n \geq 1/\alpha$. Let

$$f^{\text{LC}} = \arg \min_{f \in \mathcal{F}_d} D_{KL}(f^* \| f) = \arg \min_{f \in \mathcal{F}_d} \int_{\mathbb{R}^d} f^*(x) \log \left(\frac{f^*(x)}{f(x)} \right) dx.$$

If $f^* \in \mathcal{F}_d$, then $f^{LC} = f^*$. We write the empirical KL divergence between f^* and $\widehat{f}_{1,n}$, evaluated on $\{Y_i : i \in \mathcal{D}_{0,n}\}$, as

$$\widehat{D}_{KL}(f^* \parallel \widehat{f}_{1,n}) = \frac{1}{|\mathcal{D}_{0,n}|} \sum_{i \in \mathcal{D}_{0,n}} \log \left(\frac{f^*(Y_i)}{\widehat{f}_{1,n}(Y_i)} \right).$$

Then we can also see that $\widehat{f}_{0,n} = \arg \min_{f \in \mathcal{F}_d} \widehat{D}_{KL}(f^* \parallel f)$.

When $f^* \notin \mathcal{F}_d$, Theorem 3 establishes conditions under which the power of the universal test converges to 1 as $n \rightarrow \infty$.

Theorem 3. *We make five assumptions:*

1. *Suppose each $\widehat{f}_{1,n} \in \mathcal{C}$, where \mathcal{C} is some (potentially nonparametric) class of functions that satisfies $\sup_{f \in \mathcal{C}} |\widehat{D}_{KL}(f^* \parallel f) - D_{KL}(f^* \parallel f)| = O_P(n^{-\beta_1})$ for some $\beta_1 > 0$.*
2. *$D_{KL}(f^* \parallel \widehat{f}_{1,n}) = O_P(n^{-\beta_2})$ for some $0 < \beta_2 \leq 1/2$.*
3. *$\int_{\mathbb{R}^d} \|x\| f^*(x) dx < \infty$.*

Suppose there is some set A with $P(A) = 1$ (e.g., the support of f^{LC} or its interior) that satisfies the following:

4. *For some $\ell > 0$, $\inf_{x \in A} f^{LC}(x) \geq \ell$.*
5. *$\sup_{x \in A} |\widehat{f}_{0,n}(x) - f^{LC}(x)| \xrightarrow{a.s.} 0$.*

Then $\lim_{n \rightarrow \infty} \mathbb{P}_{H_0}(T_n \geq 1/\alpha) = 1$.

These assumptions are not very restrictive. For false positive rate control, the universal inference method does not restrict how $\widehat{f}_{1,n}$ is picked; it can be arbitrary. However, to study power, we need assumptions on $\widehat{f}_{1,n}$. The second assumption states that $\widehat{f}_{1,n}$ must in some way tend to f^* , meaning that function space that it implicitly or explicitly works in (like a reproducing kernel Hilbert space) must be relatively rich and nonparametric. The first assumption, however, states that this function space cannot be too rich — the class needs to be small enough that the empirical KL of any function to f^* uniformly approximates its true KL to f^* . The third assumption is trivially true if f^* is log-concave, but if it is not, we still need it to have a finite mean, and the fourth assumption states that its log-concave projection must be bounded away from zero.

It may be possible to drop some of these assumptions. For example, Assumption 4 may follow from Lemma 3(b) of Cule and Samworth (2010) if A is additionally a compact and convex set. Suppose X_1, X_2, \dots is an iid sequence with density f^* , the support of f^* is the smallest closed set E with $\int_E f^* = 1$, and $\text{conv}(S)$ is the convex hull of some compact subset S of the interior of E . Under our assumption 3, their Lemma 3(b) states that there is a constant $c > 0$ such that, with probability one, $\liminf_{n \rightarrow \infty} \inf_{x \in \text{conv}(S)} \widehat{f}_{0,n}(x) \geq c$. Since it is likely that $\widehat{f}_{0,n}$ converges to f^{LC} in the limit, the same property may hold for f^{LC} as well.

Similarly, Assumption 5 may hold by default if f^{LC} is continuous over A . Under our assumption 3, as well as $\int_{\mathbb{R}^d} f^* \log_+(f^*) < \infty$, $\text{int}(E) \neq \emptyset$, and continuity of f^{LC} , Theorem 3

of Cule et al. (2010) states that $\sup_{x \in \mathbb{R}^d} \exp(a\|x\|) |\widehat{f}_{0,n}(x) - f^{\text{LC}}(x)| \rightarrow 0$ almost surely as $n \rightarrow \infty$. Under assumption 4, it is impossible for f^{LC} to be continuous over \mathbb{R}^d . However, outside of A , the tails of $\widehat{f}_{0,n}$ and f^{LC} are both 0.

We provide a proof sketch to show how these five assumptions lead to the result. The full proof appears in Appendix A.

Proof sketch. We begin by separating T_n into a product of three components:

$$T_n = \underbrace{\left\{ \prod_{i \in \mathcal{D}_{0,n}} \frac{\widehat{f}_{1,n}(Y_i)}{f^*(Y_i)} \right\}}_{C_{1,n}} \underbrace{\left\{ \prod_{i \in \mathcal{D}_{0,n}} \frac{f^*(Y_i)}{f^{\text{LC}}(Y_i)} \right\}}_{C_{2,n}} \underbrace{\left\{ \prod_{i \in \mathcal{D}_{0,n}} \frac{f^{\text{LC}}(Y_i)}{\widehat{f}_{0,n}(Y_i)} \right\}}_{C_{3,n}}.$$

Define

$$\epsilon := \|(f^{\text{LC}})^{1/2} - (f^*)^{1/2}\|_2 = \left[\int ((f^{\text{LC}})^{1/2} - (f^*)^{1/2})^2 d\mu \right]^{1/2}.$$

This choice of ϵ arises from Lemma 1 of Wong and Shen (1995). We see that

$$\begin{aligned} & \mathbb{P}(T_n < 1/\alpha) \\ & \leq \mathbb{P}\left(C_{2,n} < \exp\left(\frac{n}{8}\epsilon^2\right) \cup C_{1,n} < \frac{1}{\alpha} \exp\left(-\frac{n}{16}\epsilon^2\right) \cup C_{3,n} < \exp\left(-\frac{n}{16}\epsilon^2\right)\right) \\ & \leq \mathbb{P}\left(C_{2,n} < \exp\left(\frac{n}{8}\epsilon^2\right)\right) + \mathbb{P}\left(C_{1,n} < \frac{1}{\alpha} \exp\left(-\frac{n}{16}\epsilon^2\right)\right) + \mathbb{P}\left(C_{3,n} < \exp\left(-\frac{n}{16}\epsilon^2\right)\right). \end{aligned}$$

We want to show that these three probabilities converge to 0.

Using Lemma 1 of Wong and Shen (1995), we show that

$$\mathbb{P}\left(C_{2,n} < \exp\left(\frac{n}{8}\epsilon^2\right)\right) \leq \exp\left(-\frac{n}{8}\epsilon^2\right).$$

So $\lim_{n \rightarrow \infty} \mathbb{P}(C_{2,n} < \exp((n/8)\epsilon^2)) = 0$.

For the second probability, we use assumptions 1 and 2 to show that $\log(C_{1,n}) = O_P(n^{1-\beta})$, where $\beta = \min\{\beta_1, \beta_2\} \in (0, 1/2]$. This implies that $\lim_{n \rightarrow \infty} \mathbb{P}(C_{1,n} < (1/\alpha) \exp(-(n/16)\epsilon^2)) = 0$.

For the third probability, we use Markov's inequality to derive

$$\mathbb{P}\left(C_{3,n} < \exp\left(-\frac{n}{16}\epsilon^2\right)\right) \leq \frac{8}{\epsilon^2} \mathbb{E} \left[\frac{2}{n} \sum_{i \in \mathcal{D}_{0,n}} \log\left(\frac{\widehat{f}_{0,n}(Y_i)}{f^{\text{LC}}(Y_i)}\right) \right].$$

Let $\delta > 0$. Using ℓ from assumption 4, fix $\gamma > 0$ such that $\gamma < \ell(\exp(\delta) - 1)$. Note that this implies $\log((\gamma + \ell)/\ell) < \delta$. We derive

$$\begin{aligned} \mathbb{E} \left[\frac{2}{n} \sum_{i \in \mathcal{D}_{0,n}} \log\left(\frac{\widehat{f}_{0,n}(Y_i)}{f^{\text{LC}}(Y_i)}\right) \right] & < \mathbb{E} \left[\frac{2}{n} \sum_{i \in \mathcal{D}_{0,n}} \log(\gamma + f^{\text{LC}}(Y_i)) \right] - \mathbb{E} \left[\frac{2}{n} \sum_{i \in \mathcal{D}_{0,n}} \log(f^{\text{LC}}(Y_i)) \right] + \\ & \mathbb{E} \left[\frac{2}{n} \sum_{i \in \mathcal{D}_{0,n}} \log(\widehat{f}_{0,n}(Y_i)) I\left(\sup_{x \in A} |\widehat{f}_{0,n}(x) - f^{\text{LC}}(x)| \geq \gamma\right) \right]. \end{aligned}$$

We consider the difference of the first two expectations. The function $g(x) = \log(\gamma + x) - \log(x)$ is a decreasing function, so $g(x)$ is maximized at the smallest x . By assumption 4, we know that with probability 1, $f^{\text{LC}}(Y_i) \geq \ell$. This tells us that

$$\mathbb{E} \left[\frac{2}{n} \sum_{i \in \mathcal{D}_{0,n}} \log(\gamma + f^{\text{LC}}(Y_i)) \right] - \mathbb{E} \left[\frac{2}{n} \sum_{i \in \mathcal{D}_{0,n}} \log(f^{\text{LC}}(Y_i)) \right] \leq \log(\gamma + \ell) - \log(\ell) < \delta.$$

By Lemma 3(a) of Cule and Samworth (2010), assumption 3 implies that for some $u > 0$, $\limsup_{n \rightarrow \infty} \sup_{x \in \mathbb{R}^d} \widehat{f}_{0,n}(x) \leq u$ with probability 1. Using reverse Fatou's Lemma for conditional expectations, we determine

$$\begin{aligned} & \limsup_{n \rightarrow \infty} \mathbb{E} \left[\frac{2}{n} \sum_{i \in \mathcal{D}_{0,n}} \log(\widehat{f}_{0,n}(Y_i)) I \left(\sup_{x \in A} |\widehat{f}_{0,n}(x) - f^{\text{LC}}(x)| \geq \gamma \right) \right] \\ & \leq u \mathbb{P} \left(\sup_{x \in A} |\widehat{f}_{0,n}(x) - f^{\text{LC}}(x)| \geq \gamma \right) \quad \text{with probability 1.} \end{aligned}$$

Finally, by assumption 5, $\lim_{n \rightarrow \infty} \mathbb{P} \left(\sup_{x \in A} |\widehat{f}_{0,n}(x) - f^{\text{LC}}(x)| \geq \gamma \right) \rightarrow 0$. So with probability 1, for arbitrary $\delta > 0$,

$$\lim_{n \rightarrow \infty} \mathbb{E} \left[\frac{2}{n} \sum_{i \in \mathcal{D}_{0,n}} \log \left(\frac{\widehat{f}_{0,n}(Y_i)}{f^{\text{LC}}(Y_i)} \right) \right] < \delta.$$

We conclude that $\lim_{n \rightarrow \infty} \mathbb{P} \left(C_{3,n} < \exp \left(-\frac{n}{16} \epsilon^2 \right) \right) = 0$. Therefore, $\lim_{n \rightarrow \infty} \mathbb{P}(T_n < 1/\alpha) = 0$. \square

6 Conclusion

We have implemented and evaluated several universal LRTs to test for log-concavity. These methods provide the first tests for log-concavity that are valid in finite samples under only the assumption that the data sample is iid. The tests include a full oracle (true density) approach, a partial oracle (parametric) approach, a fully nonparametric approach, and several LRTs that reduce the d -dimensional test to a set of one-dimensional tests. For reference, we compared these tests to a permutation test although that test is not guaranteed to be valid. In one dimension, the universal tests can have higher power than the permutation test. In higher dimensions, we have seen that the permutation test can falsely reject H_0 at a rate much higher than α . In contrast, the universal tests are still valid in higher dimensions. As seen in the Gaussian mixture case, the dimension reduction universal approaches can have notably stronger performance than the universal tests that work with d -dimensional densities.

Several open questions remain. Theorem 3 presented a set of conditions under which the universal LRT has power that converges to 1 as $n \rightarrow \infty$. As discussed, it may be possible to weaken some of these conditions. In addition, future work may seek to theoretically derive

the power as a function of the dimension, number of observations, and signal strength. As shown in one example (Figure 13 of Appendix B), the signal may need to grow exponentially in d to maintain the same power.

Acknowledgements

RD is currently employed at Novartis Pharmaceuticals Corporation. This work was conducted while RD was at Carnegie Mellon University. RD’s research was supported by the National Science Foundation Graduate Research Fellowship Program under Grant Nos. DGE 1252522 and DGE 1745016. AR’s research is supported by the Adobe Faculty Research Award, an ARL Large Grant, and the National Science Foundation under Grant Nos. DMS 2053804, DMS 1916320, and DMS (CAREER) 1945266. Any opinions, findings, and conclusions or recommendations expressed in this material are those of the authors and do not necessarily reflect the views of the National Science Foundation. This work used the Extreme Science and Engineering Discovery Environment (XSEDE) (Townsend et al., 2014), which is supported by National Science Foundation grant number ACI-1548562. Specifically, it used the Bridges system (Nystrom et al., 2015), which is supported by NSF award number ACI-1445606, at the Pittsburgh Supercomputing Center (PSC). This work made extensive use of the R statistical software (R Core Team, 2021), as well as the `data.table` (Dowle and Srinivasan, 2021), `fitdistrplus` (Delignette-Muller and Dutang, 2015), `kde1d` (Nagler and Vatter, 2020), `ks` (Duong, 2021), `LogConcDEAD` (Cule et al., 2009), `logcondens` (Dümbgen and Rufibach, 2011), `MASS` (Venables and Ripley, 2002), `mclust` (Scrucca et al., 2016), `mvtnorm` (Genz et al., 2021; Genz and Bretz, 2009), and `tidyverse` (Wickham et al., 2019) packages.

References

- Mark Yuying An. Log-concave probability distributions: Theory and statistical testing. *Duke University Dept of Economics Working Paper*, (95-03), 1997.
- Mark Bagnoli and Ted Bergstrom. Log-concave probability and its applications. *Economic Theory*, 26(2):445–469, 2005.
- Adrian W Bowman. An alternative method of cross-validation for the smoothing of density estimates. *Biometrika*, 71(2):353–360, 1984.
- Raymond J Carroll, Aurore Delaigle, and Peter Hall. Testing and estimating shape-constrained nonparametric density and regression in the presence of measurement error. *Journal of the American Statistical Association*, 106(493):191–202, 2011.
- José E Chacón and Tarn Duong. Multivariate plug-in bandwidth selection with unconstrained pilot bandwidth matrices. *Test*, 19(2):375–398, 2010.
- Wenyu Chen, Rahul Mazumder, and Richard Samworth. A new computational framework for log-concave density estimation. *arXiv preprint arXiv:2105.11387*, 2021.

- Yining Chen and Richard J Samworth. Smoothed log-concave maximum likelihood estimation with applications. *Statistica Sinica*, 23:1373–1398, 2013.
- Madeleine Cule and Richard Samworth. Theoretical properties of the log-concave maximum likelihood estimator of a multidimensional density. *Electronic Journal of Statistics*, 4: 254–270, 2010.
- Madeleine Cule, Robert Gramacy, and Richard Samworth. LogConcDEAD: An R package for maximum likelihood estimation of a multivariate log-concave density. *Journal of Statistical Software*, 29(2):1–20, 2009.
- Madeleine Cule, Richard Samworth, and Michael Stewart. Maximum likelihood estimation of a multi-dimensional log-concave density. *Journal of the Royal Statistical Society: Series B (Statistical Methodology)*, 72(5):545–607, 2010.
- Marie Laure Delignette-Muller and Christophe Dutang. fitdistrplus: An R package for fitting distributions. *Journal of Statistical Software*, 64(4):1–34, 2015.
- Matt Dowle and Arun Srinivasan. *data.table: Extension of ‘data.frame’*, 2021. R package version 1.14.2.
- Lutz Dümbgen and Kaspar Rufibach. logcondens: Computations related to univariate log-concave density estimation. *Journal of Statistical Software*, 39(6):1–28, 2011.
- Lutz Dümbgen, André Hüsler, and Kaspar Rufibach. Active set and EM algorithms for log-concave densities based on complete and censored data. *arXiv preprint arXiv:0707.4643*, 2007.
- Tarn Duong. *ks: Kernel Smoothing*, 2021. R package version 1.13.2.
- Tarn Duong and Martin Hazelton. Plug-in bandwidth matrices for bivariate kernel density estimation. *Journal of Nonparametric Statistics*, 15(1):17–30, 2003.
- Tarn Duong and Martin L Hazelton. Cross-validation bandwidth matrices for multivariate kernel density estimation. *Scandinavian Journal of Statistics*, 32(3):485–506, 2005.
- Alan Genz and Frank Bretz. *Computation of Multivariate Normal and t Probabilities*. Lecture Notes in Statistics. Springer-Verlag, Heidelberg, 2009. ISBN 978-3-642-01688-2.
- Alan Genz, Frank Bretz, Tetsuhisa Miwa, Xuefei Mi, Friedrich Leisch, Fabian Scheipl, and Torsten Hothorn. *mvtnorm: Multivariate Normal and t Distributions*, 2021. R package version 1.1-3.
- Martin L Hazelton. Assessing log-concavity of multivariate densities. *Statistics & Probability Letters*, 81(1):121–125, 2011.
- MC Jones, James Stephen Marron, and Byeong U Park. A simple root n bandwidth selector. *The Annals of Statistics*, 19(4):1919–1932, 1991.

- Franz Kappel and Alexei V Kuntsevich. An implementation of Shor’s r-algorithm. *Computational Optimization and Applications*, 15(2):193–205, 2000.
- Arlene KH Kim and Richard J Samworth. Global rates of convergence in log-concave density estimation. *Annals of Statistics*, 44(6):2756–2779, 2016.
- Roger Koenker and Ivan Mizera. Shape constrained density estimation via penalized Rényi divergence. *Statistical Science*, 33(4):510–526, 2018.
- Gil Kur, Yuval Dagan, and Alexander Rakhlin. Optimality of maximum likelihood for log-concave density estimation and bounded convex regression. *arXiv preprint arXiv:1903.05315*, 2019.
- Thomas Nagler and Thibault Vatter. *kde1d: Univariate Kernel Density Estimation*, 2020. R package version 1.13.2.
- Nicholas A Nystrom, Michael J Levine, Ralph Z Roskies, and J Ray Scott. Bridges: A uniquely flexible HPC resource for new communities and data analytics. In *Proceedings of the 2015 XSEDE Conference: Scientific Advancements Enabled by Enhanced Cyberinfrastructure*, XSEDE ’15, pages 1–8, New York, NY, USA, 2015. Association for Computing Machinery. ISBN 9781450337205. doi: 10.1145/2792745.2792775.
- András Prékopa. On logarithmic concave measures and functions. *Acta Scientiarum Mathematicarum*, 34:335–343, 1973.
- R Core Team. *R: A Language and Environment for Statistical Computing*. R Foundation for Statistical Computing, Vienna, Austria, 2021.
- Mats Rudemo. Empirical choice of histograms and kernel density estimators. *Scandinavian Journal of Statistics*, 9(2):65–78, 1982.
- Luca Scrucca, Michael Fop, T. Brendan Murphy, and Adrian E. Raftery. mclust 5: Clustering, classification and density estimation using Gaussian finite mixture models. *The R Journal*, 8(1):289–317, 2016.
- Naum Zuselevich Shor. *Minimization methods for non-differentiable functions*, volume 3. Springer Science & Business Media, 2012.
- Grzegorz Sitek. The modes of a mixture of two normal distributions. *Silesian Journal of Pure and Applied Mathematics*, 6(1):59–67, 2016.
- J. Towns, T. Cockerill, M. Dahan, I. Foster, K. Gaither, A. Grimshaw, V. Hazlewood, S. Lathrop, D. Lifka, G. D. Peterson, R. Roskies, J. R. Scott, and N. Wilkins-Diehr. XSEDE: Accelerating scientific discovery. *Computing in Science & Engineering*, 16(5): 62–74, Sept.-Oct. 2014. ISSN 1521-9615. doi: 10.1109/MCSE.2014.80.
- W. N. Venables and B. D. Ripley. *Modern Applied Statistics with S*. Springer, New York, fourth edition, 2002. ISBN 0-387-95457-0.

- Matt P Wand and M Chris Jones. Multivariate plug-in bandwidth selection. *Computational Statistics*, 9(2):97–116, 1994.
- Larry Wasserman, Aaditya Ramdas, and Sivaraman Balakrishnan. Universal inference. *Proceedings of the National Academy of Sciences*, 117(29):16880–16890, 2020.
- Hadley Wickham, Mara Averick, Jennifer Bryan, Winston Chang, Lucy D’Agostino McGowan, Romain François, Garrett Golemund, Alex Hayes, Lionel Henry, Jim Hester, Max Kuhn, Thomas Lin Pedersen, Evan Miller, Stephan Milton Bache, Kirill Müller, Jeroen Ooms, David Robinson, Dana Paige Seidel, Vitalie Spinu, Kohske Takahashi, Davis Vaughan, Claus Wilke, Kara Woo, and Hiroaki Yutani. Welcome to the tidyverse. *Journal of Open Source Software*, 4(43):1686, 2019. doi: 10.21105/joss.01686.
- Wing Hung Wong and Xiaotong Shen. Probability inequalities for likelihood ratios and convergence rates of sieve MLEs. *The Annals of Statistics*, 23(2):339–362, 1995.

A Proofs of Theoretical Results

Theorem 1 (Wasserman et al. (2020)). $T_n(\widehat{f}_0)$ is an e -value, meaning that it has expectation at most one under the null. Hence, $1/T_n(\widehat{f}_0)$ is a valid p -value, and rejecting the null when $T_n(\widehat{f}_0) \geq 1/\alpha$ is a valid level- α test. That is, under $H_0 : f^* \in \mathcal{F}_d$,

$$\mathbb{P}(T_n(\widehat{f}_0) \geq 1/\alpha) \leq \alpha.$$

Proof. This result is due to Wasserman et al. (2020). First, we use only the data $\{Y_i : i \in \mathcal{D}_1\}$ to fit a density \widehat{f}_1 . Let \mathcal{M}^* be the support of the distribution P^* with density f^* , and let $\widehat{\mathcal{M}}_1$ be the support of the distribution with density \widehat{f}_1 . We see

$$\begin{aligned} \mathbb{E}_{P^*} [T_n(f^*) \mid \{Y_i\}_{i \in \mathcal{D}_1}] &= \mathbb{E}_{P^*} \left[\frac{\mathcal{L}_0(\widehat{f}_1)}{\mathcal{L}_0(f^*)} \mid \{Y_i\}_{i \in \mathcal{D}_1} \right] = \mathbb{E}_{P^*} \left[\prod_{i \in \mathcal{D}_0} \frac{\widehat{f}_1(Y_i)}{f^*(Y_i)} \mid \{Y_i\}_{i \in \mathcal{D}_1} \right] \\ &\stackrel{iid}{=} \prod_{i \in \mathcal{D}_0} \mathbb{E}_{P^*} \left[\frac{\widehat{f}_1(Y_i)}{f^*(Y_i)} \mid \{Y_i\}_{i \in \mathcal{D}_1} \right] = \prod_{i \in \mathcal{D}_0} \left\{ \int_{\mathcal{M}^*} \frac{\widehat{f}_1(y_i)}{f^*(y_i)} f^*(y_i) dy_i \right\} = \prod_{i \in \mathcal{D}_0} \left\{ \int_{\mathcal{M}^*} \widehat{f}_1(y_i) dy_i \right\} \\ &\leq \prod_{i \in \mathcal{D}_0} \left\{ \int_{\widehat{\mathcal{M}}_1} \widehat{f}_1(y_i) dy_i \right\} = 1. \end{aligned}$$

This implies that $\mathbb{E}_{P^*}[T_n(f^*)] = \mathbb{E}_{P^*}[\mathbb{E}_{P^*}[T_n(f^*) \mid \{Y_i\}_{i \in \mathcal{D}_1}]] \leq 1$. Furthermore, recall that $T_n(f^*) = \mathcal{L}_0(\widehat{f}_1)/\mathcal{L}_0(f^*)$ and $T_n(\widehat{f}_0) = \mathcal{L}_0(\widehat{f}_1)/\mathcal{L}_0(\widehat{f}_0)$, where $\widehat{f}_0 = \arg \max_{f \in \mathcal{F}_d} \mathcal{L}_0(f)$. Thus,

under $H_0 : f^* \in \mathcal{F}_d$, it holds that $T_n(\widehat{f}_0) \leq T_n(f^*)$ and $\mathbb{E}_{P^*}[T_n(\widehat{f}_0)] \leq 1$.

Applying Markov's inequality and the above fact, under H_0 ,

$$\mathbb{P}_{P^*} \left(T_n(\widehat{f}_0) \geq 1/\alpha \right) \leq \alpha \mathbb{E}_{P^*}[T_n(\widehat{f}_0)] \leq \alpha.$$

□

Fact 1. For $\gamma \in (0, 1)$, the normal location mixture $f(x) = \gamma\phi_d(x) + (1 - \gamma)\phi_d(x - \mu)$ is log-concave only when $\|\mu\| \leq 2$.

Proof. In the one-dimensional setting,

$$f(x; \mu) = \frac{\gamma}{\sqrt{2\pi}} \exp\left(-\frac{1}{2}x^2\right) + \frac{1 - \gamma}{\sqrt{2\pi}} \exp\left(-\frac{1}{2}(x - \mu)^2\right).$$

We define $\ell(x; \mu) \equiv \log(f(x; \mu))$. We wish to show that $\frac{\partial^2}{\partial x^2} \ell(x; \mu) \leq 0$ for all x iff $\|\mu\| \leq 2$.

We derive

$$\begin{aligned} \frac{\partial}{\partial x} \ell(x; \mu) &= \frac{1}{f(x; \mu)} \left(\frac{\partial}{\partial x} f(x; \mu) \right) \\ &= \frac{1}{f(x; \mu)} \left(-x f(x; \mu) + \frac{\mu(1 - \gamma)}{\sqrt{2\pi}} \exp\left(-\frac{1}{2}(x - \mu)^2\right) \right) \\ &= -x + \frac{\mu(1 - \gamma)}{f(x; \mu)\sqrt{2\pi}} \exp\left(-\frac{1}{2}(x - \mu)^2\right). \end{aligned}$$

Then

$$\begin{aligned}
& \frac{\partial^2}{\partial x^2} \ell(x; \mu) \\
&= -1 + \frac{\mu(\mu - x)(1 - \gamma)}{f(x; \mu)\sqrt{2\pi}} \exp\left(-\frac{1}{2}(x - \mu)^2\right) - \frac{\mu(1 - \gamma)\sqrt{2\pi}(\partial f(x; \mu)/\partial x)}{(f(x; \mu)\sqrt{2\pi})^2} \exp\left(-\frac{1}{2}(x - \mu)^2\right) \\
&= -1 + \frac{\mu(\mu - x)(1 - \gamma)}{f(x; \mu)\sqrt{2\pi}} \exp\left(-\frac{1}{2}(x - \mu)^2\right) - \\
&\quad \frac{\mu(1 - \gamma)\sqrt{2\pi}[-xf(x; \mu) + \mu(1 - \gamma)\exp(-\frac{1}{2}(x - \mu)^2)/\sqrt{2\pi}]}{(f(x; \mu)\sqrt{2\pi})^2} \exp\left(-\frac{1}{2}(x - \mu)^2\right) \\
&= -1 + \frac{\mu(\mu - x)(1 - \gamma)}{f(x; \mu)\sqrt{2\pi}} \exp\left(-\frac{1}{2}(x - \mu)^2\right) + \\
&\quad \frac{\mu x(1 - \gamma)}{f(x; \mu)\sqrt{2\pi}} \exp\left(-\frac{1}{2}(x - \mu)^2\right) - \frac{\mu^2(1 - \gamma)^2}{(f(x; \mu)\sqrt{2\pi})^2} \exp(-(x - \mu)^2) \\
&= -1 + \frac{\mu^2(1 - \gamma)}{f(x; \mu)\sqrt{2\pi}} \exp\left(-\frac{1}{2}(x - \mu)^2\right) - \frac{\mu^2(1 - \gamma)^2}{(f(x; \mu)\sqrt{2\pi})^2} \exp(-(x - \mu)^2).
\end{aligned}$$

Then the following statements are equivalent:

$$\text{For all } x \in \mathbb{R}, 0 \geq \frac{\partial^2}{\partial x^2} \ell(x; \mu). \quad (1)$$

$$\text{For all } x \in \mathbb{R}, 0 \geq -(f(x; \mu)\sqrt{2\pi})^2 + \mu^2(1 - \gamma)f(x; \mu)\sqrt{2\pi} \exp\left(-\frac{1}{2}(x - \mu)^2\right) - \mu^2(1 - \gamma)^2 \exp(-(x - \mu)^2).$$

$$\text{For all } x \in \mathbb{R}, 0 \geq -\left(\gamma \exp\left(-\frac{1}{2}x^2\right) + (1 - \gamma) \exp\left(-\frac{1}{2}(x - \mu)^2\right)\right)^2 + \mu^2(1 - \gamma) \exp\left(-\frac{1}{2}(x - \mu)^2\right) \left(\gamma \exp\left(-\frac{1}{2}x^2\right) + (1 - \gamma) \exp\left(-\frac{1}{2}(x - \mu)^2\right)\right) - \mu^2(1 - \gamma)^2 \exp(-(x - \mu)^2).$$

$$\text{For all } x \in \mathbb{R}, 0 \geq -\left(\gamma \exp\left(-\frac{1}{2}x^2\right) + (1 - \gamma) \exp\left(-\frac{1}{2}(x - \mu)^2\right)\right)^2 + \mu^2(1 - \gamma)\gamma \exp\left(-\frac{1}{2}(x - \mu)^2\right) \exp\left(-\frac{1}{2}x^2\right).$$

$$\text{For all } x \in \mathbb{R}, 0 \geq -\gamma^2 \exp(-x^2) - 2\gamma(1 - \gamma) \exp\left(-\frac{1}{2}x^2\right) \exp\left(-\frac{1}{2}(x - \mu)^2\right) - (1 - \gamma)^2 \exp(-(x - \mu)^2) + \mu^2(1 - \gamma)\gamma \exp\left(-\frac{1}{2}x^2\right) \exp\left(-\frac{1}{2}(x - \mu)^2\right).$$

$$\text{For all } x \in \mathbb{R}, \mu^2 \leq 2 + \frac{\gamma}{1 - \gamma} \exp\left(-\frac{1}{2}x^2\right) \exp\left(\frac{1}{2}(x - \mu)^2\right) + \frac{1 - \gamma}{\gamma} \exp\left(\frac{1}{2}x^2\right) \exp\left(-\frac{1}{2}(x - \mu)^2\right).$$

$$\text{For all } x \in \mathbb{R}, \mu^2 \leq 2 + \frac{\gamma}{1 - \gamma} \exp\left(-x\mu + \frac{1}{2}\mu^2\right) + \frac{1 - \gamma}{\gamma} \exp\left(x\mu - \frac{1}{2}\mu^2\right).$$

Let us define $g(x; \mu) = 2 + \frac{\gamma}{1-\gamma} \exp(-x\mu + \frac{1}{2}\mu^2) + \frac{1-\gamma}{\gamma} \exp(x\mu - \frac{1}{2}\mu^2)$. We can show that $g(x; \mu)$ is minimized at $x = \frac{\mu}{2} + \frac{1}{2\mu} \log(\gamma^2/(1-\gamma)^2)$. Then (1) is equivalent to the following:

$$\begin{aligned} \mu^2 &\leq 2 + \frac{\gamma}{1-\gamma} \exp\left(-\frac{1}{2}\mu^2 - \frac{1}{2} \log\left(\frac{\gamma^2}{(1-\gamma)^2}\right) + \frac{1}{2}\mu^2\right) + \\ &\quad \frac{1-\gamma}{\gamma} \exp\left(\frac{1}{2}\mu^2 + \frac{1}{2} \log\left(\frac{\gamma^2}{(1-\gamma)^2}\right) - \frac{1}{2}\mu^2\right). \\ \mu^2 &\leq 2 + \frac{\gamma}{1-\gamma} \exp\left(\frac{1}{2} \log\left(\frac{(1-\gamma)^2}{\gamma^2}\right)\right) + \frac{1-\gamma}{\gamma} \exp\left(\frac{1}{2} \log\left(\frac{\gamma^2}{(1-\gamma)^2}\right)\right). \\ \mu^2 &\leq 4. \end{aligned}$$

We conclude that $f(x; \mu)$ is log-concave if and only if $|\mu| \leq 2$. The extension to d dimensions follows by Proposition 1 of Cule et al. (2010). □

Theorem 3. *We make five assumptions:*

1. Suppose each $\widehat{f}_{1,n} \in \mathcal{C}$, where \mathcal{C} is some (potentially nonparametric) class of functions that satisfies $\sup_{f \in \mathcal{C}} |\widehat{D}_{KL}(f^*||f) - D_{KL}(f^*||f)| = O_P(n^{-\beta_1})$ for some $\beta_1 > 0$.
2. $D_{KL}(f^*||\widehat{f}_{1,n}) = O_P(n^{-\beta_2})$ for some $0 < \beta_2 \leq 1/2$.
3. $\int_{\mathbb{R}^d} \|x\| f^*(x) dx < \infty$.

Suppose there is some set A with $P(A) = 1$ (e.g., the support of f^{LC} or its interior) that satisfies the following:

4. For some $\ell > 0$, $\inf_{x \in A} f^{LC}(x) \geq \ell$.
5. $\sup_{x \in A} |\widehat{f}_{0,n}(x) - f^{LC}(x)| \xrightarrow{a.s.} 0$.

Then $\lim_{n \rightarrow \infty} \mathbb{P}_{H_0}(T_n \geq 1/\alpha) = 1$.

Proof. We begin by separating T_n into a product of three components:

$$T_n = \underbrace{\left\{ \prod_{i \in \mathcal{D}_{0,n}} \frac{\widehat{f}_{1,n}(Y_i)}{f^*(Y_i)} \right\}}_{C_{1,n}} \underbrace{\left\{ \prod_{i \in \mathcal{D}_{0,n}} \frac{f^*(Y_i)}{f^{LC}(Y_i)} \right\}}_{C_{2,n}} \underbrace{\left\{ \prod_{i \in \mathcal{D}_{0,n}} \frac{f^{LC}(Y_i)}{\widehat{f}_{0,n}(Y_i)} \right\}}_{C_{3,n}}.$$

Define ϵ as

$$\epsilon = \|(f^{LC})^{1/2} - (f^*)^{1/2}\|_2 = \left[\int ((f^{LC})^{1/2} - (f^*)^{1/2})^2 d\mu \right]^{1/2}.$$

We see that

$$\begin{aligned} &\mathbb{P}(T_n < 1/\alpha) \\ &\leq \mathbb{P}\left(C_{2,n} < \exp\left(\frac{n}{8}\epsilon^2\right) \cup C_{1,n} < \frac{1}{\alpha} \exp\left(-\frac{n}{16}\epsilon^2\right) \cup C_{3,n} < \exp\left(-\frac{n}{16}\epsilon^2\right)\right) \\ &\leq \mathbb{P}\left(C_{2,n} < \exp\left(\frac{n}{8}\epsilon^2\right)\right) + \mathbb{P}\left(C_{1,n} < \frac{1}{\alpha} \exp\left(-\frac{n}{16}\epsilon^2\right)\right) + \mathbb{P}\left(C_{3,n} < \exp\left(-\frac{n}{16}\epsilon^2\right)\right). \end{aligned}$$

We want to show that these three probabilities converge to 0.

By Lemma 1 of Wong and Shen (1995), we can see

$$\begin{aligned}
\mathbb{P}\left(C_{2,n} < \exp\left(\frac{n}{8}\epsilon^2\right)\right) &= \mathbb{P}\left(\prod_{i \in \mathcal{D}_{0,n}} \frac{f^*(Y_i)}{f^{\text{LC}}(Y_i)} < \exp\left(\frac{n}{8}\epsilon^2\right)\right) \\
&= \mathbb{P}\left(\prod_{i \in \mathcal{D}_{0,n}} \frac{f^{\text{LC}}(Y_i)}{f^*(Y_i)} > \exp\left(-\frac{n}{8}\epsilon^2\right)\right) \\
&\leq \exp\left(-\frac{n}{8}\epsilon^2\right).
\end{aligned}$$

So $\lim_{n \rightarrow \infty} \mathbb{P}(C_{2,n} < \exp((n/8)\epsilon^2)) = 0$.

For the second probability, we use assumptions 1 and 2 to see that

$$\begin{aligned}
\log(C_{1,n}) &= \log\left(\prod_{i \in \mathcal{D}_{0,n}} \frac{\hat{f}_{1,n}(Y_i)}{f^*(Y_i)}\right) \\
&= \sum_{i \in \mathcal{D}_{0,n}} \log\left(\frac{\hat{f}_{1,n}(Y_i)}{f^*(Y_i)}\right) \\
&= -\frac{n}{2} \cdot \frac{2}{n} \sum_{i \in \mathcal{D}_{0,n}} \log\left(\frac{f^*(Y_i)}{\hat{f}_{1,n}(Y_i)}\right) \\
&= -\frac{n}{2} \hat{D}_{KL}(f^* \| \hat{f}_{1,n}) \\
&= -\frac{n}{2} \left(\hat{D}_{KL}(f^* \| \hat{f}_{1,n}) - D_{KL}(f^* \| \hat{f}_{1,n})\right) - \frac{n}{2} D_{KL}(f^* \| \hat{f}_{1,n}) \\
&= -\frac{n}{2} O_P(n^{-\beta_1}) - \frac{n}{2} O_P(n^{-\beta_2}) \\
&= O_P(n^{1-\beta}),
\end{aligned}$$

where $\beta = \min\{\beta_1, \beta_2\} \in (0, 1/2]$. We fix $M > 0$ such that $\lim_{n \rightarrow \infty} \mathbb{P}(|\log(C_{1,n})/n^{1-\beta}| > M) = 0$.

We see that

$$\begin{aligned}
& \mathbb{P}(C_{1,n} < (1/\alpha) \exp(-(n/16)\epsilon^2)) \\
&= \mathbb{P}(\log(C_{1,n}) < \log(1/\alpha) - (n/16)\epsilon^2) \\
&= \mathbb{P}(\log(C_{1,n}) < \log(1/\alpha) - (n/16)\epsilon^2, \log(C_{1,n}) \geq 0) + \\
&\quad \mathbb{P}(\log(C_{1,n}) < \log(1/\alpha) - (n/16)\epsilon^2, \log(C_{1,n}) < 0) \\
&\leq \mathbb{P}(\log(1/\alpha) - (n/16)\epsilon^2 > 0) + \mathbb{P}(-|\log(C_{1,n})| < \log(1/\alpha) - (n/16)\epsilon^2) \\
&= \mathbb{P}(\log(1/\alpha) - (n/16)\epsilon^2 > 0) + \mathbb{P}(|\log(C_{1,n})| > (n/16)\epsilon^2 - \log(1/\alpha)) \\
&= \mathbb{P}(\log(1/\alpha) - (n/16)\epsilon^2 > 0) + \mathbb{P}(|\log(C_{1,n})/n^{1-\beta}| > (n^\beta/16)\epsilon^2 - n^{\beta-1} \log(1/\alpha)) \\
&= \mathbb{P}(\log(1/\alpha) - (n/16)\epsilon^2 > 0) + \\
&\quad \mathbb{P}(|\log(C_{1,n})/n^{1-\beta}| > (n^\beta/16)\epsilon^2 - n^{\beta-1} \log(1/\alpha), (n^\beta/16)\epsilon^2 - n^{\beta-1} \log(1/\alpha) > M) + \\
&\quad \mathbb{P}(|\log(C_{1,n})/n^{1-\beta}| > (n^\beta/16)\epsilon^2 - n^{\beta-1} \log(1/\alpha), (n^\beta/16)\epsilon^2 - n^{\beta-1} \log(1/\alpha) \leq M) \\
&\leq \mathbb{P}(\log(1/\alpha) - (n/16)\epsilon^2 > 0) + \mathbb{P}(|\log(C_{1,n})/n^{1-\beta}| > M) + \mathbb{P}((n^\beta/16)\epsilon^2 \leq n^{\beta-1} \log(1/\alpha) + M) \\
&\leq \mathbb{P}(\log(1/\alpha) - (n/16)\epsilon^2 > 0) + \mathbb{P}(|\log(C_{1,n})/n^{1-\beta}| > M) + \mathbb{P}((n^\beta/16)\epsilon^2 \leq \log(1/\alpha) + M).
\end{aligned}$$

We know that $\lim_{n \rightarrow \infty} \mathbb{P}(\log(1/\alpha) - (n/16)\epsilon^2 > 0) = 0$, $\lim_{n \rightarrow \infty} \mathbb{P}(|\log(C_{1,n})/n^{1-\beta}| > M) = 0$, and $\lim_{n \rightarrow \infty} \mathbb{P}((n^\beta/16)\epsilon^2 \leq \log(1/\alpha) + M) = 0$. We conclude that

$$\lim_{n \rightarrow \infty} \mathbb{P}(C_{1,n} < (1/\alpha) \exp(-(n/16)\epsilon^2)) = 0.$$

For the third probability, we see that

$$\begin{aligned}
\mathbb{P}\left(C_{3,n} < \exp\left(-\frac{n}{16}\epsilon^2\right)\right) &= \mathbb{P}\left(\log\left(\prod_{i \in \mathcal{D}_{0,n}} \frac{f^{\text{LC}}(Y_i)}{\widehat{f}_{0,n}(Y_i)}\right) < -\frac{n}{16}\epsilon^2\right) \\
&= \mathbb{P}\left(\sum_{i \in \mathcal{D}_{0,n}} \log\left(\frac{\widehat{f}_{0,n}(Y_i)}{f^{\text{LC}}(Y_i)}\right) > \frac{n}{16}\epsilon^2\right) \\
&= \mathbb{P}\left(\frac{2}{n} \sum_{i \in \mathcal{D}_{0,n}} \log\left(\frac{\widehat{f}_{0,n}(Y_i)}{f^{\text{LC}}(Y_i)}\right) > \frac{1}{8}\epsilon^2\right) \\
&\leq \frac{8}{\epsilon^2} \mathbb{E}\left[\frac{2}{n} \sum_{i \in \mathcal{D}_{0,n}} \log\left(\frac{\widehat{f}_{0,n}(Y_i)}{f^{\text{LC}}(Y_i)}\right)\right].
\end{aligned}$$

Note that Markov's inequality applies in the final step because $\widehat{f}_{0,n}$ and f^{LC} are both log-concave densities, and $\widehat{f}_{0,n}$ maximizes the likelihood over all log-concave densities on $\mathcal{D}_{0,n}$. This means that the quantity within the expectation is nonnegative. Let $\delta > 0$. Using ℓ from assumption 4, fix $\gamma > 0$ such that $\gamma < \ell(\exp(\delta) - 1)$. Note that this implies $\log((\gamma + \ell)/\ell) < \delta$. Then

$$\begin{aligned}
& \mathbb{E} \left[\frac{2}{n} \sum_{i \in \mathcal{D}_{0,n}} \log \left(\frac{\widehat{f}_{0,n}(Y_i)}{f^{\text{LC}}(Y_i)} \right) \right] \\
&= \mathbb{E} \left[\frac{2}{n} \sum_{i \in \mathcal{D}_{0,n}} \log(\widehat{f}_{0,n}(Y_i)) \right] - \mathbb{E} \left[\frac{2}{n} \sum_{i \in \mathcal{D}_{0,n}} \log(f^{\text{LC}}(Y_i)) \right] \\
&= \mathbb{E} \left[\left\{ \frac{2}{n} \sum_{i \in \mathcal{D}_{0,n}} \log(\widehat{f}_{0,n}(Y_i)) \right\} \left\{ I \left(\sup_{x \in A} |\widehat{f}_{0,n}(x) - f^{\text{LC}}(x)| < \gamma \right) + I \left(\sup_{x \in A} |\widehat{f}_{0,n}(x) - f^{\text{LC}}(x)| \geq \gamma \right) \right\} \right] - \\
&\quad \mathbb{E} \left[\frac{2}{n} \sum_{i \in \mathcal{D}_{0,n}} \log(f^{\text{LC}}(Y_i)) \right] \\
&= \mathbb{E} \left[\left\{ \frac{2}{n} \sum_{i \in \mathcal{D}_{0,n}} \log(\widehat{f}_{0,n}(Y_i) - f^{\text{LC}}(Y_i) + f^{\text{LC}}(Y_i)) \right\} I \left(\sup_{x \in A} |\widehat{f}_{0,n}(x) - f^{\text{LC}}(x)| < \gamma \right) \right] + \\
&\quad \mathbb{E} \left[\frac{2}{n} \sum_{i \in \mathcal{D}_{0,n}} \log(\widehat{f}_{0,n}(Y_i)) I \left(\sup_{x \in A} |\widehat{f}_{0,n}(x) - f^{\text{LC}}(x)| \geq \gamma \right) \right] - \mathbb{E} \left[\frac{2}{n} \sum_{i \in \mathcal{D}_{0,n}} \log(f^{\text{LC}}(Y_i)) \right] \\
&< \mathbb{E} \left[\frac{2}{n} \sum_{i \in \mathcal{D}_{0,n}} \log(\gamma + f^{\text{LC}}(Y_i)) \right] - \mathbb{E} \left[\frac{2}{n} \sum_{i \in \mathcal{D}_{0,n}} \log(f^{\text{LC}}(Y_i)) \right] + \\
&\quad \mathbb{E} \left[\frac{2}{n} \sum_{i \in \mathcal{D}_{0,n}} \log(\widehat{f}_{0,n}(Y_i)) I \left(\sup_{x \in A} |\widehat{f}_{0,n}(x) - f^{\text{LC}}(x)| \geq \gamma \right) \right] \tag{2} \\
&\leq \log(\gamma + \ell) - \log(\ell) + \mathbb{E} \left[\frac{2}{n} \sum_{i \in \mathcal{D}_{0,n}} \log(\widehat{f}_{0,n}(Y_i)) I \left(\sup_{x \in A} |\widehat{f}_{0,n}(x) - f^{\text{LC}}(x)| \geq \gamma \right) \right] \tag{3} \\
&< \delta + \mathbb{E} \left[\frac{2}{n} \sum_{i \in \mathcal{D}_{0,n}} \log(\widehat{f}_{0,n}(Y_i)) I \left(\sup_{x \in A} |\widehat{f}_{0,n}(x) - f^{\text{LC}}(x)| \geq \gamma \right) \right].
\end{aligned}$$

Step (2) to step (3) holds because $g(x) = \log(\gamma + x) - \log(x)$ is a decreasing function, so $g(x)$ is maximized at the smallest x . By assumption 4, we know that with probability 1, $f^{\text{LC}}(Y_i) \geq \ell$, so setting $x = \ell$ provides an upper bound.

By Lemma 3(a) of Cule and Samworth (2010), assumption 3 implies that for some $u > 0$, $\limsup_{n \rightarrow \infty} \sup_{x \in \mathbb{R}^d} \widehat{f}_{0,n}(x) \leq u$ with probability 1. Using reverse Fatou's Lemma for

conditional expectations in step (4), we see

$$\begin{aligned}
& \limsup_{n \rightarrow \infty} \mathbb{E} \left[\frac{2}{n} \sum_{i \in \mathcal{D}_{0,n}} \log(\widehat{f}_{0,n}(Y_i)) I \left(\sup_{x \in A} |\widehat{f}_{0,n}(x) - f^{\text{LC}}(x)| \geq \gamma \right) \right] \\
&= \limsup_{n \rightarrow \infty} \mathbb{E} \left[\frac{2}{n} \sum_{i \in \mathcal{D}_{0,n}} \log(\widehat{f}_{0,n}(Y_i)) \mid \sup_{x \in A} |\widehat{f}_{0,n}(x) - f^{\text{LC}}(x)| \geq \gamma \right] \mathbb{P} \left(\sup_{x \in A} |\widehat{f}_{0,n}(x) - f^{\text{LC}}(x)| \geq \gamma \right) \\
&\leq \limsup_{n \rightarrow \infty} \mathbb{E} \left[\sup_{x \in \mathbb{R}^d} (\log(\widehat{f}_{0,n}(x))) \mid \sup_{x \in A} |\widehat{f}_{0,n}(x) - f^{\text{LC}}(x)| \geq \gamma \right] \mathbb{P} \left(\sup_{x \in A} |\widehat{f}_{0,n}(x) - f^{\text{LC}}(x)| \geq \gamma \right) \\
&\leq \limsup_{n \rightarrow \infty} \mathbb{E} \left[\sup_{x \in \mathbb{R}^d} (\widehat{f}_{0,n}(x)) \mid \sup_{x \in A} |\widehat{f}_{0,n}(x) - f^{\text{LC}}(x)| \geq \gamma \right] \mathbb{P} \left(\sup_{x \in A} |\widehat{f}_{0,n}(x) - f^{\text{LC}}(x)| \geq \gamma \right) \\
&\leq \mathbb{E} \left[\limsup_{n \rightarrow \infty} \sup_{x \in \mathbb{R}^d} (\widehat{f}_{0,n}(x)) \mid \sup_{x \in A} |\widehat{f}_{0,n}(x) - f^{\text{LC}}(x)| \geq \gamma \right] \mathbb{P} \left(\sup_{x \in A} |\widehat{f}_{0,n}(x) - f^{\text{LC}}(x)| \geq \gamma \right) \\
&\leq u \mathbb{P} \left(\sup_{x \in A} |\widehat{f}_{0,n}(x) - f^{\text{LC}}(x)| \geq \gamma \right) \quad \text{with probability 1.}
\end{aligned} \tag{4}$$

Finally, by assumption 5, $\lim_{n \rightarrow \infty} \mathbb{P} \left(\sup_{x \in A} |\widehat{f}_{0,n}(x) - f^{\text{LC}}(x)| \geq \gamma \right) \rightarrow 0$. So with probability 1, for arbitrary $\delta > 0$,

$$\lim_{n \rightarrow \infty} \mathbb{E} \left[\frac{2}{n} \sum_{i \in \mathcal{D}_{0,n}} \log \left(\frac{\widehat{f}_{0,n}(Y_i)}{f^{\text{LC}}(Y_i)} \right) \right] < \delta.$$

We conclude that $\lim_{n \rightarrow \infty} \mathbb{P} \left(C_{3,n} < \exp \left(-\frac{n}{16} \epsilon^2 \right) \right) = 0$. Therefore, $\lim_{n \rightarrow \infty} \mathbb{P}_{H_0} (T_n < 1/\alpha) = 0$. \square

B Additional Normal Mixture Simulations

B.1 Visualizing Log-concave MLEs

In Section 2, we visualize the log-concave MLEs of samples from two-component Gaussian mixtures of the form

$$f^*(x) = 0.5\phi_d(x) + 0.5\phi_d(x - \mu).$$

Section 2 considers the $n = 5000$ and $d = 1$ setting for both log-concave ($\|\mu\| \leq 2$) and not log-concave ($\|\mu\| > 2$) true densities. We provide visualizations in several additional settings.

In the one-dimensional setting, we compute the log-concave MLEs \widehat{f}_n on samples $\{x_1, \dots, x_n\}$. Figures 6 and 7 show the true and log-concave MLE densities for samples with $n = 50$ and $n = 5000$, respectively. These simulations use both the `LogConcDEAD` and `logcondens` packages. `logcondens` only works in one dimension but is much faster than `LogConcDEAD`. Visually, we see that these two packages produce approximately the same densities. Furthermore,

we include values of $n^{-1} \sum_{i=1}^n \log(f^*(x_i))$ on the true density plots and $n^{-1} \sum_{i=1}^n \log(\hat{f}_n(x_i))$ on the log-concave MLE plots. The log likelihood is approximately the same for the two density estimation methods.

When $\|\mu\| = 0$ or $\|\mu\| = 2$, the true density is log-concave. As we increase from $n = 50$ to $n = 5000$, the log-concave MLE becomes a better approximation to the true density. We see this improvement both visually and numerically. That is, $n^{-1} \sum_{i=1}^n \log(\hat{f}_n(x_i))$ is closer to $n^{-1} \sum_{i=1}^n \log(f^*(x_i))$ for larger n . When $\|\mu\| = 4$, the underlying density is not log-concave. The log-concave MLE at $\|\mu\| = 4$ and $n = 5000$ seems to have normal tails, but it is nearly uniform in the middle.

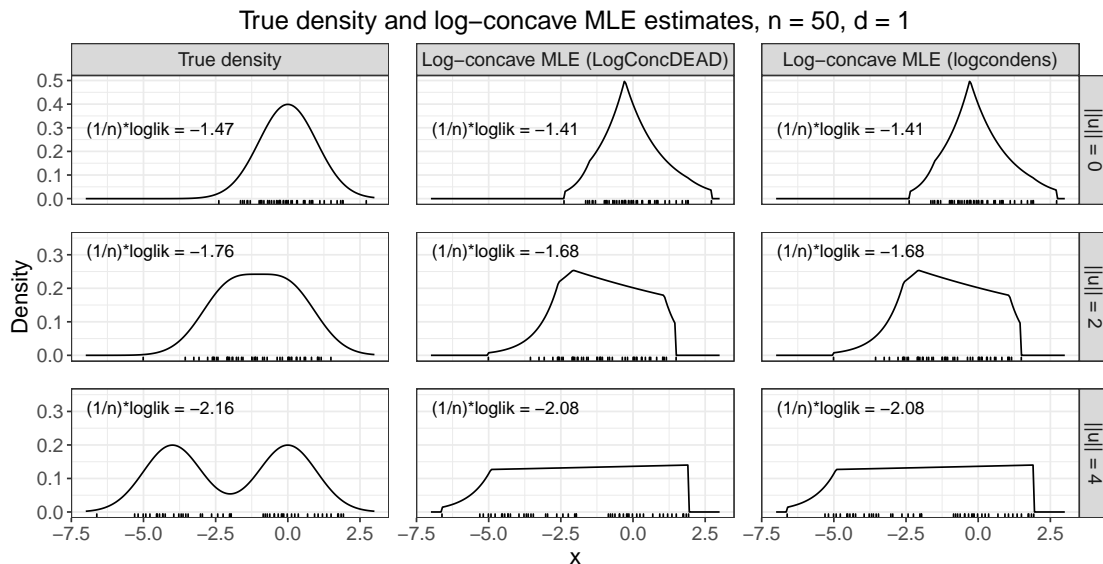


Figure 6: Density plots from fitting log-concave MLE on $n = 50$ observations. Tick marks represent the observations. The true density is the Normal mixture $f^*(x) = 0.5\phi_1(x) + 0.5\phi_1(x - \mu)$. In all settings, the LogConcDEAD and logcondens packages return similar results.

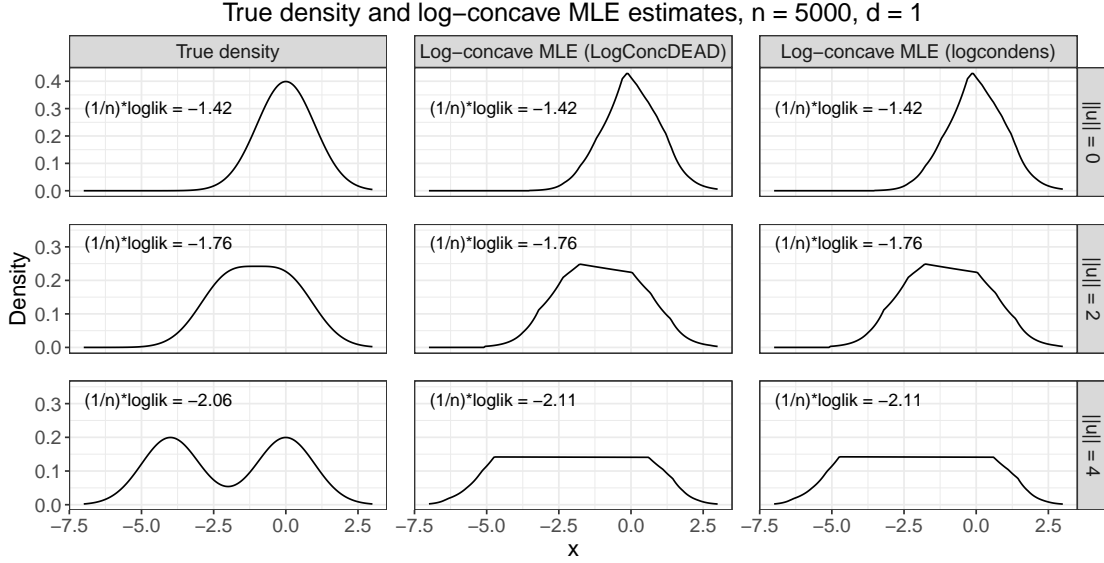


Figure 7: Density plots from fitting log-concave MLE on $n = 5000$ observations. The true density is the Normal mixture $f^*(x) = 0.5\phi_1(x) + 0.5\phi_1(x - \mu)$. In all settings, the LogConcDEAD and logcondens packages return similar results. In the $\|\mu\| = 0$ and $\|\mu\| = 2$ log-concave settings, the log-concave MLE on 5000 observations is close to the true density. In the $\|\mu\| = 4$ non-log-concave setting, the log-concave densities appear to have normal tails and uniform centers.

We observe similar behavior in the two-dimensional setting. In two dimensions, we use $\mu = (-\|\mu\|, 0)$. Figures 8 and 9 show two-dimensional contour plots for the true and log-concave MLEs with $n = 50$ and $n = 500$. In Figure 8, we can clearly see that the support of the log-concave MLE is the convex hull of the observed sample. For $\|\mu\| = 0$ and $\|\mu\| = 2$, the true density and log-concave MLE have more similar appearances when $n = 500$. In addition, $n^{-1} \sum_{i=1}^n \log(\hat{f}_n(x_i))$ is closer to $n^{-1} \sum_{i=1}^n \log(f^*(x_i))$ for larger n . When $\|\mu\| = 4$, the log-concave MLE density is nearly flat in the center of the density.

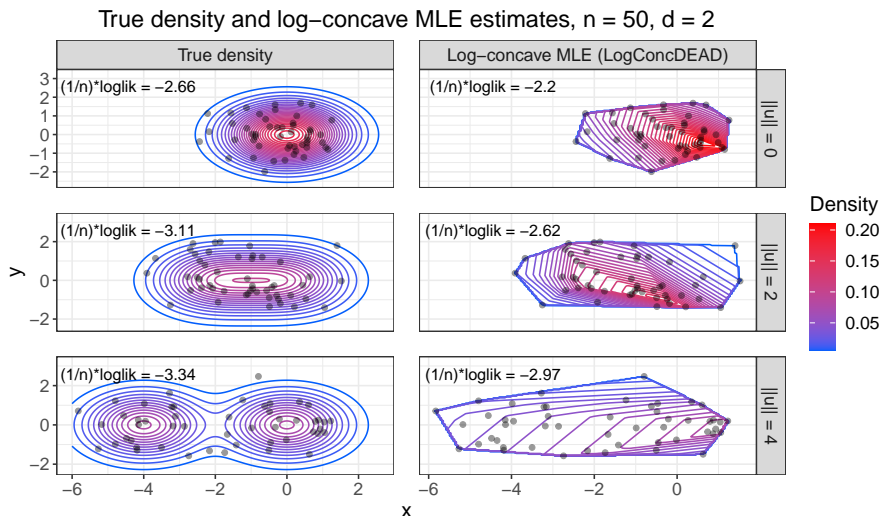


Figure 8: Contour plots from fitting log-concave MLE on $n = 50$ observations. Points represent the 50 observations. The true density is the Normal mixture $f^*(x) = 0.5\phi_2(x) + 0.5\phi_2(x - \mu)$. The log-concave MLE has a density of zero outside of the convex hull of the observations.

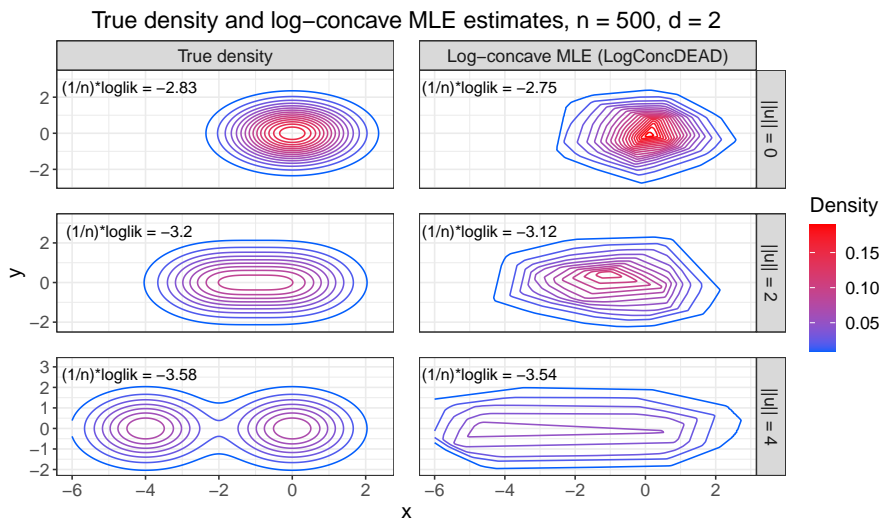


Figure 9: Contour plots from fitting log-concave MLE on $n = 500$ observations. The true density is the Normal mixture $f^*(x) = 0.5\phi_2(x) + 0.5\phi_2(x - \mu)$. In the $\|\mu\| = 0$ and $\|\mu\| = 2$ settings, the log-concave MLE over 500 observations has a similar appearance to the true density. When $\|\mu\| = 4$, the interior of the log-concave MLE density appears to be nearly uniform, similar to the $d = 1$ case.

B.2 Permutation Test under Additional Parameter Settings

Figure 1 demonstrated that the permutation test for log-concavity was not valid for $d \geq 4$ at $n = 100$. We consider whether these results still hold with a larger sample size. Figure 10

simulates the permutation test at $n = 250$. Compared to the $n = 100$ setting, this setting has slightly higher power at $\|\mu\| = 4$ and $\|\mu\| = 5$ when $d = 1$ or $d = 2$. We still see that the rejection proportion is much higher than 0.10 for $\|\mu\| \leq 2$ at $d = 4$ and $d = 5$.

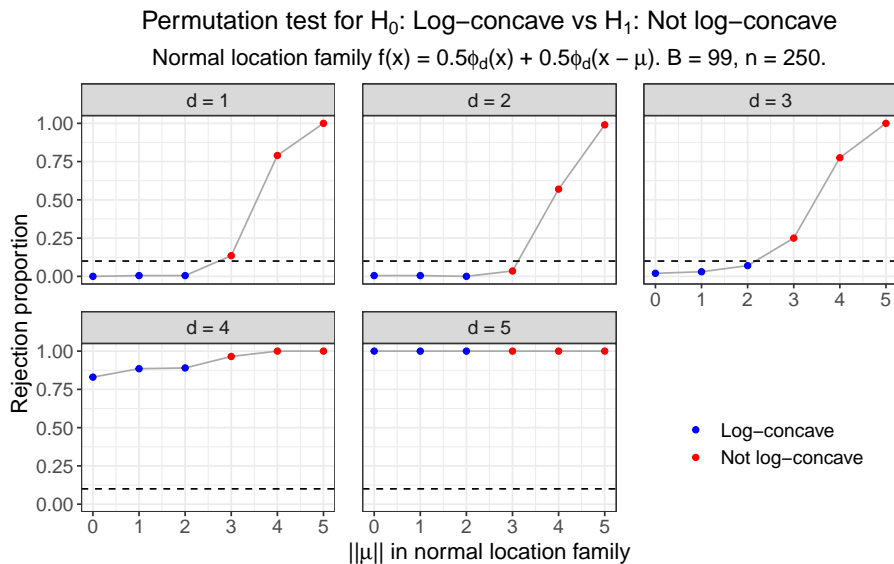


Figure 10: Rejection proportions for test of $H_0 : f^*$ is log-concave versus $H_1 : f^*$ is not log-concave, using the permutation test from Cule et al. (2010). We set $\alpha = 0.10$ and $n = 250$, and we perform 200 simulations at each combination of $(d, \|\mu\|)$. The test permutes the observations $B = 99$ times. The results are similar to the permutation test results of Figure 1. The permutation test is valid or approximately valid for $d \leq 3$, but it is not valid for $d \geq 4$.

Next, we consider whether the permutation test results hold if we increase B , the number of times that we shuffle the sample. In Figure 11, we show the results of simulations at $B \in \{100, 200, 300, 400, 500\}$ on $n = 100$ observations. Each row corresponds to the same set of simulations performed at five values of B . Looking across each row, we do not see an effect as B increases from 100 to 500. In these analyses, the lack of validity at $d = 4$ and $d = 5$ remains as we increase n or increase B .

Permutation test for H_0 : Log-concave vs H_1 : Not log-concave

Normal location family $f(x) = 0.5\phi_d(x) + 0.5\phi_d(x - \mu)$. Varying B . $n = 100$.

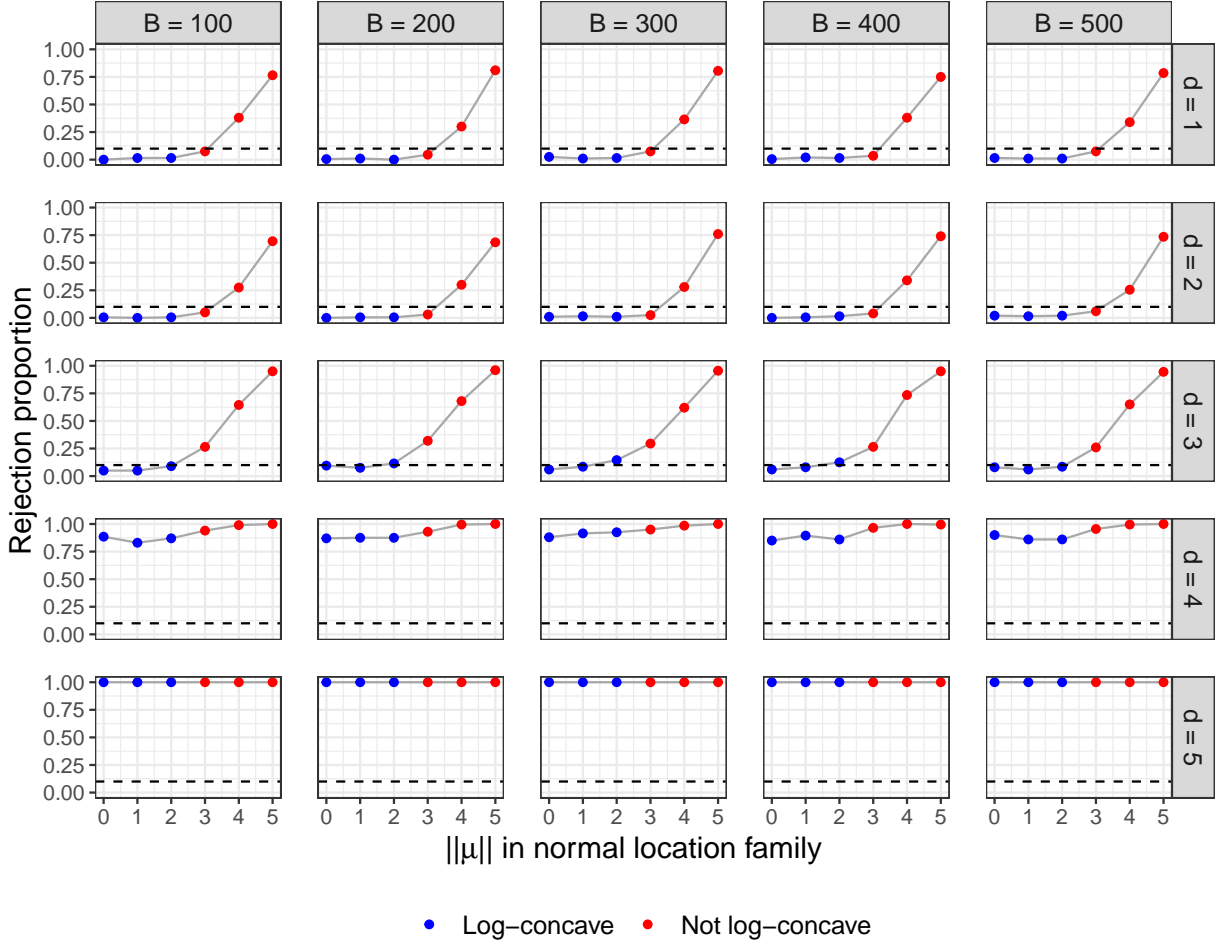


Figure 11: Rejection proportions for test of $H_0 : f^*$ is log-concave versus $H_1 : f^*$ is not log-concave, using the permutation test from Cule et al. (2010). We set $\alpha = 0.10$ and $n = 100$, and we perform 200 simulations at each combination of $(B, d, \|\mu\|)$. At these larger numbers of shuffles B , the permutation test still is not valid for $d \geq 4$.

Recall that the test statistic is $T = \sup_{A \in \mathcal{A}_0} |P_n(A) - P_n^*(A)|$, and the test statistic on a shuffled sample is $T_b^* = \sup_{A \in \mathcal{A}_0} |P_{n,b}(A) - P_{n,b}^*(A)|$. Both P and P^* are proportions (out of n observations), so T and T_b^* can only take on finitely many values. We consider whether the conservativeness of the test (e.g., $d = 1$) or the lack of validity of test (e.g., $d = 5$) is due to this discrete nature. Figure 12 plots the distribution of shuffled test statistics T_b^* across eight simulations. The left panels consider the $d = 1$ case at all combinations of $\|\mu\| \in \{0, 2\}$ and $B \in \{100, 500\}$. We see that “bunching” of the quantiles is not responsible for the test being conservative in this case. (For instance, if the 90th percentile were equal to the 99th percentile, then it would make sense for the method to be conservative at $\alpha = 0.10$.) Instead, the 0.90, 0.95, and 0.99 quantiles (dashed blue lines) are all distinct, and the original test statistic (solid black line) is less than each of these values. We also consider the behavior

in the $d = 5$ case (right panels). Again, these three quantiles are all distinct. In this case, though, the original test statistic is in the far right tail of the distribution of shuffled data test statistics.

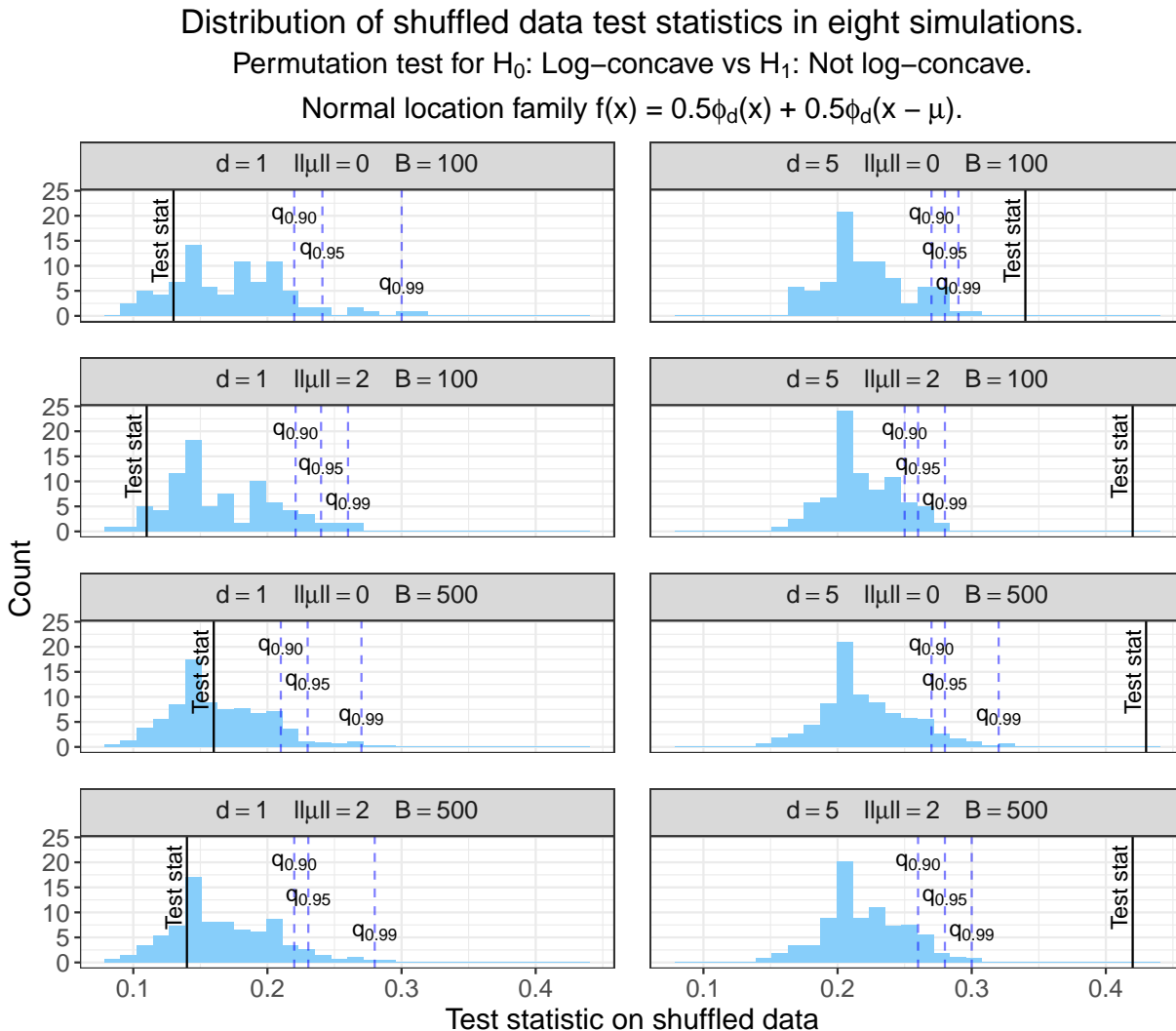


Figure 12: Distribution of $T_{n,b}^*$ across eight simulations. The dashed blue lines correspond to the quantiles of the distribution of shuffled data test statistics. The solid black lines correspond to the original test statistics in each simulation. We note that the conservative nature of the permutation test at $d = 1$ and the anticonservative nature of the permutation test at $d = 5$ are not due to the discreteness of the test statistics.

B.3 Relationship between power, $\|\mu\|$, and d in Full Oracle Test

Unlike the permutation test, the full oracle universal test controls the type I error both theoretically and in simulations. In Section 4.1, we note that $\|\mu\|$ needs to grow exponentially with d to maintain a certain level of power in the full oracle test. Figure 13 demonstrates this relationship, by exploring how $\|\mu\|$ needs to grow with d to maintain power of approximately

0.90. For each value of d , we vary $\|\mu\|$ in increments of 1 and estimate the power through 200 simulations. We choose the value of $\|\mu\|$ with power closest to 0.90. If none of the $\|\mu\|$ values have power in the range of $[0.88, 0.92]$ at a given d , then we use finer-grained values of $\|\mu\|$. From the best fit curve, it appears that $\|\mu\|$ needs to grow at an exponential rate in d to maintain the same power. Thus, while the full oracle approach offers an improvement in validity over the permutation test, the power becomes substantially worse in higher dimensions.

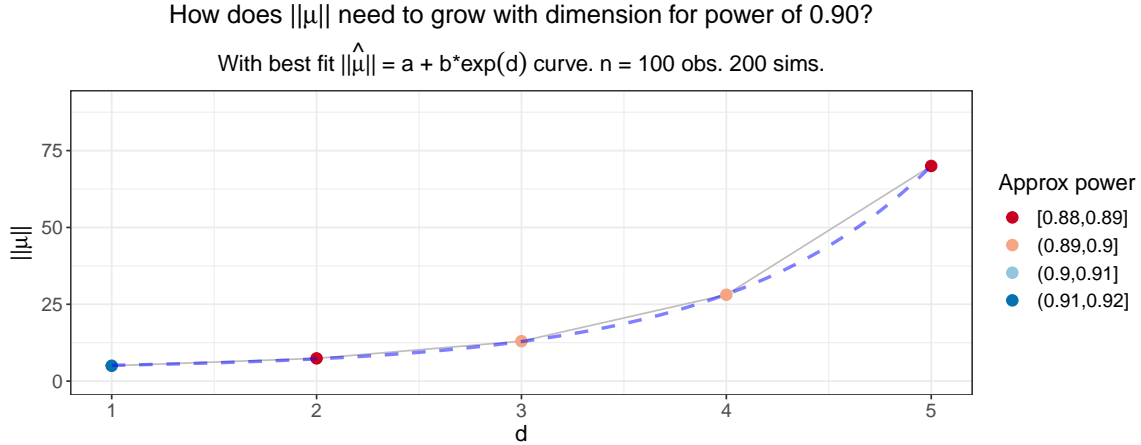


Figure 13: Power of the universal test of $H_0 : f^*$ is log-concave versus $H_1 : f^*$ is not log-concave. Simulations use the true density numerator, $B = 100$ subsamples, and $n = 100$ observations. $\|\mu\|$ needs to grow exponentially in d to maintain power of 0.90.

C Example: Testing Log-concavity of Beta Density

In the one-dimensional normal mixture case, we saw that the full oracle universal test sometimes had higher power than the permutation test. We consider whether this holds in another one-dimensional setting.

The Beta(α, β) density has the form

$$f(x; \alpha, \beta) = \frac{\Gamma(\alpha + \beta)}{\Gamma(\alpha)\Gamma(\beta)} x^{\alpha-1} (1-x)^{\beta-1}, \quad x \in (0, 1),$$

where $\alpha > 0$ and $\beta > 0$ are shape parameters.

As noted in Cule et al. (2010), Beta(α, β) is log-concave if $\alpha \geq 1$ and $\beta \geq 1$. We can see this in a quick derivation:

$$\begin{aligned} \frac{\partial^2}{\partial x^2} \log f(x; \alpha, \beta) &= \frac{\partial^2}{\partial x^2} \left[\log \left(\frac{\Gamma(\alpha + \beta)}{\Gamma(\alpha)\Gamma(\beta)} \right) + (\alpha - 1) \log(x) + (\beta - 1) \log(1 - x) \right] \\ &= \frac{\partial}{\partial x} \left[\frac{\alpha - 1}{x} + \frac{1 - \beta}{1 - x} \right] \\ &= \frac{1 - \alpha}{x^2} + \frac{1 - \beta}{(1 - x)^2}. \end{aligned}$$

This second derivative is less than or equal to 0 for all $x \in (0, 1)$ only if both $\alpha \geq 1$ and $\beta \geq 1$. The Beta(α, β) distribution is hence log-concave when $\alpha \geq 1$ and $\beta \geq 1$. This means that tests of $H_0 : f^*$ is log-concave versus $H_1 : f^*$ is not log-concave should reject H_0 if $\alpha < 1$ or $\beta < 1$.

C.1 Understanding Limiting Log-concave MLEs

In general, it is non-trivial to solve for the limiting log-concave function $f^{\text{LC}} = \arg \min_{f \in \mathcal{F}_d} D_{\text{KL}}(f^* \| f)$.

We try to determine f^{LC} in a few specific cases. In Figure 14, we consider two choices of shape parameters (α, β) such that the Beta(α, β) densities are not log-concave. On the left panels, we plot the Beta densities. For the right panels, we simulate 100,000 observations from the corresponding Beta(α, β) density, we fit the log-concave MLE on the sample using `logcondens`, and we plot this log-concave MLE density. Thus, the right panels should be good approximations to f^{LC} in these two settings.

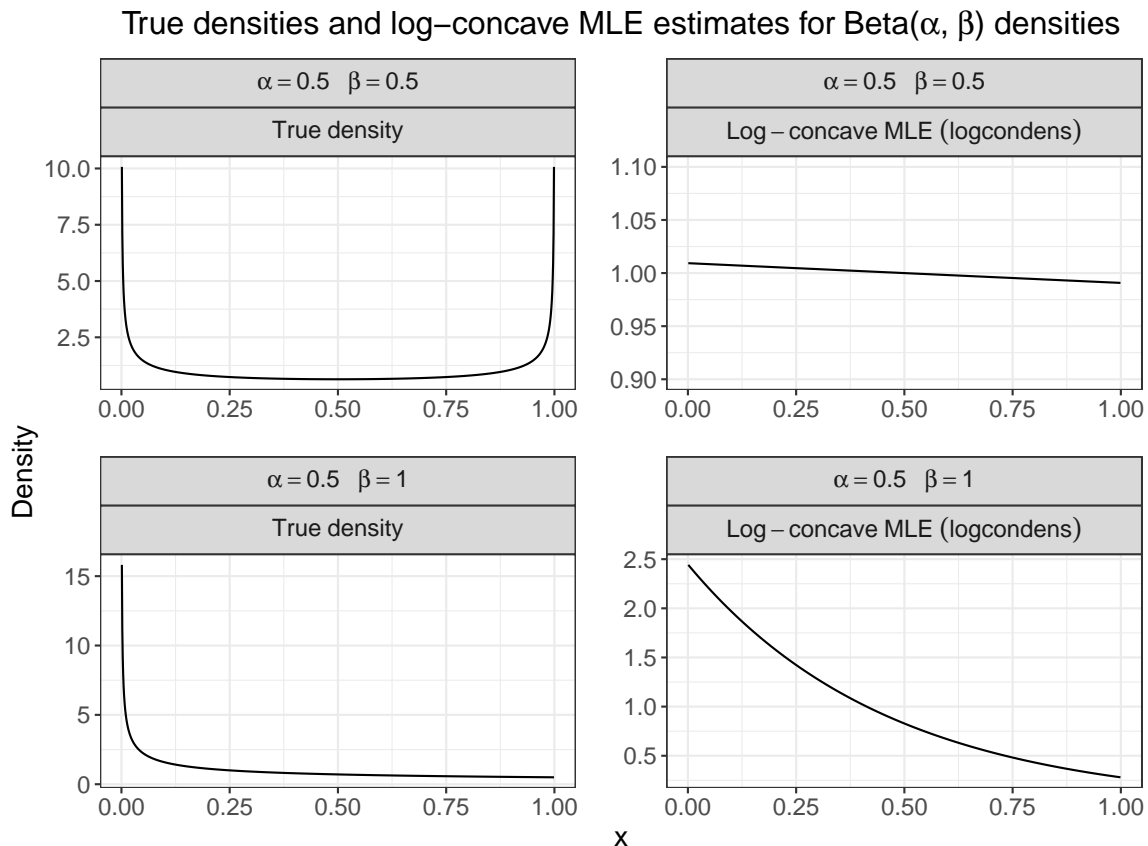


Figure 14: Two non-log-concave Beta densities and their corresponding log-concave MLEs, as estimated over $n = 100,000$ observations. The limiting log-concave MLE of the Beta(0.5, 0.5) density appears to be Unif(0, 1). The limiting log-concave MLE of the Beta(0.5, 1) density has an exponential appearance, which Figure 15 examines.

In the first setting ($\alpha = 0.5, \beta = 0.5$), it appears that the log-concave MLE is the Unif(0,

1) density. We consider the second setting ($\alpha = 0.5, \beta = 1$) in more depth. The density in row 2, column 2 looks similar to an exponential density, but x can only take on values between 0 and 1. The truncated exponential density is given by

$$f(x; \lambda, b) = \frac{\lambda \exp(-\lambda x)}{1 - \exp(-\lambda b)}, \quad 0 < x \leq b.$$

In this setting, we can try to fit a truncated exponential density with $b = 1$. In Figure 15, we see that a truncated exponential density with $\lambda = 2.18$ and $b = 1$ provides a good fit for the log-concave MLE.

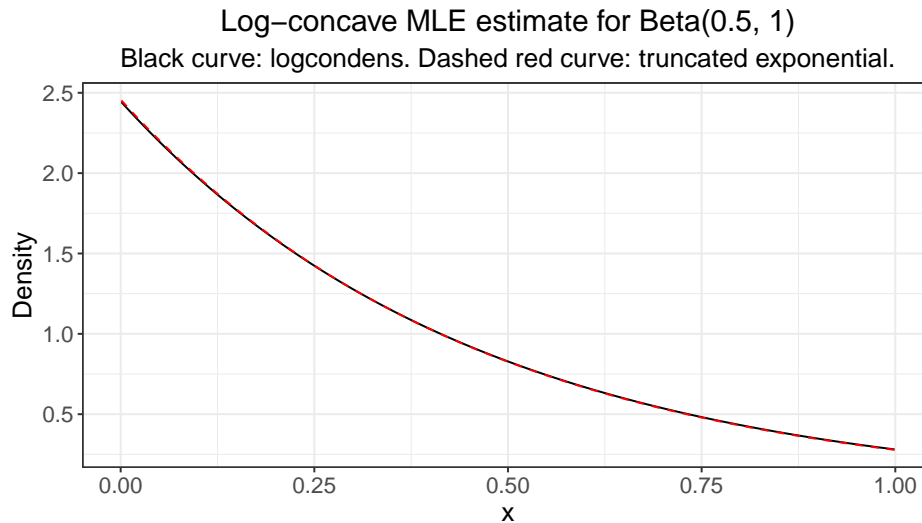


Figure 15: The log-concave MLE (black solid) estimated over $n = 100,000$ observations from the Beta(0.5, 1) density nearly perfectly matches the truncated exponential density with $\lambda = 2.18$ and $b = 1$ (red dashed). This suggests that this truncated exponential density may be the limiting log-concave MLE for this Beta density.

We can also see that the truncated exponential density is log-concave:

$$\begin{aligned} \frac{\partial^2}{\partial x^2} \log f(x; \lambda, b) &= \frac{\partial^2}{\partial x^2} [\log(\lambda) - \lambda x - \log(1 - \exp(-\lambda b))] \\ &= \frac{\partial}{\partial x} [-\lambda] \\ &= 0. \end{aligned}$$

C.2 Universal Tests can have Higher Power than Permutations

Figure 16 shows examples of both log-concave and not log-concave Beta densities. We use similar α and β parameters in the simulations where we test for log-concavity. This shows that our simulations are capturing a variety of Beta density shapes.

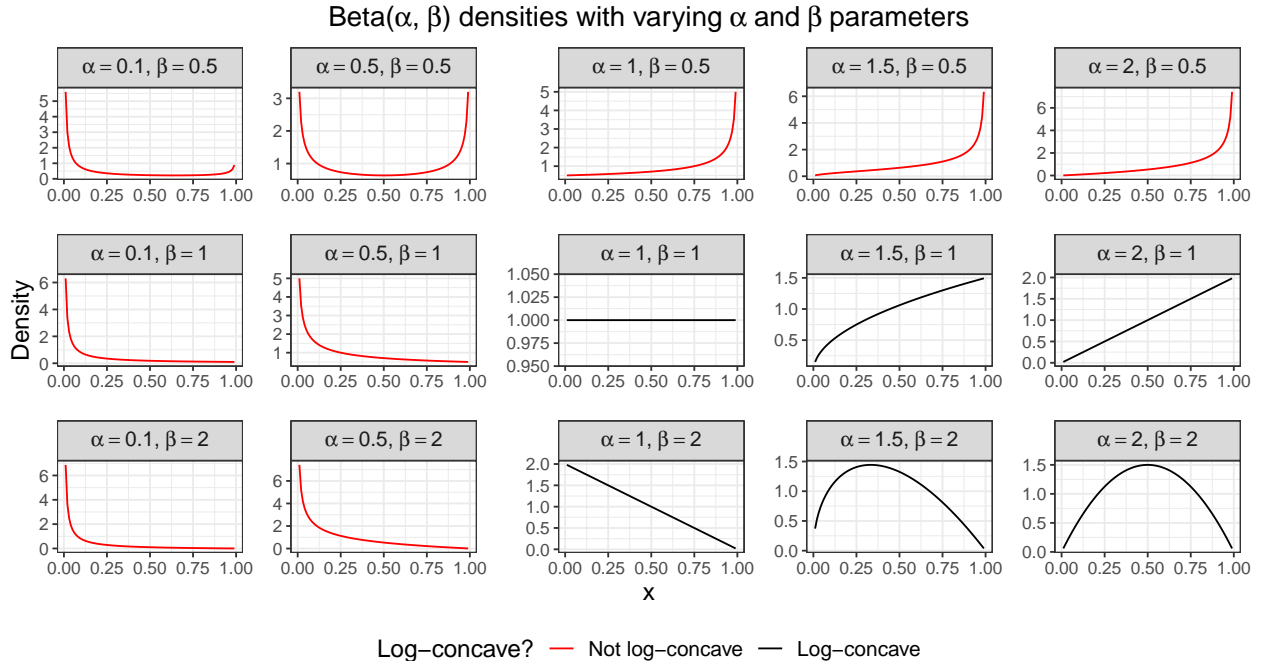


Figure 16: Beta densities across a variety of α and β parameters. We implement our log-concavity tests on Beta densities across these ranges of parameters, encompassing a variety of density shapes.

We now implement the full oracle LRT (universal), partial oracle LRT (universal), fully nonparametric LRT (universal), and permutation test. The full oracle LRT uses the true density in the numerator. The partial oracle LRT uses the knowledge that the true density comes from the Beta family. We use the `fitdist` function in the `fitdistrplus` library to find the MLE for α and β on $\{Y_i : i \in \mathcal{D}_1\}$ computationally (Delignette-Muller and Dutang, 2015). Then the numerator of the partial oracle LRT uses this Beta MLE density. The fully nonparametric approach fits a kernel density estimate on $\{Y_i : i \in \mathcal{D}_1\}$. In particular, we use the `kde1d` function from the `kde1d` library, and we restrict the support of the KDE to $[0, 1]$ (Nagler and Vatter, 2020). This restriction is particularly important in the Beta family case, since some of the non-log-concave Beta densities assign high probability to observations near 0 or 1. (See Figure 16.) The numerator of the fully nonparametric approach uses the KDE.

Figure 17 compares the four tests of $H_0 : f^*$ is log-concave versus $H_1 : f^*$ is not log-concave. We set $n = 100$, and we perform 200 simulations to determine each rejection proportion. The universal methods subsample at $B = 100$, and the permutation test uses $B = 99$ shuffles. In the first panel, $\beta = 0.5$, so the density is not log-concave for any choice of α . In the second and third panels, $\beta = 1$ and $\beta = 2$. In these cases, the density is log-concave only when $\alpha \geq 1$ as well.

We observe that the permutation test is valid in all settings, but the three universal tests often have higher power. As expected, out of the universal tests, the full oracle approach has the highest power, followed by the partial oracle approach and then the fully nonparametric approach. When $\beta = 0.5$, all of the universal LRTs have power greater than or equal to the permutation test. When $\beta \in \{1, 2\}$, the universal approaches have higher power for some

values of α . Again, we see that even when the permutation test is valid, it is possible for universal LRTs to have higher power.

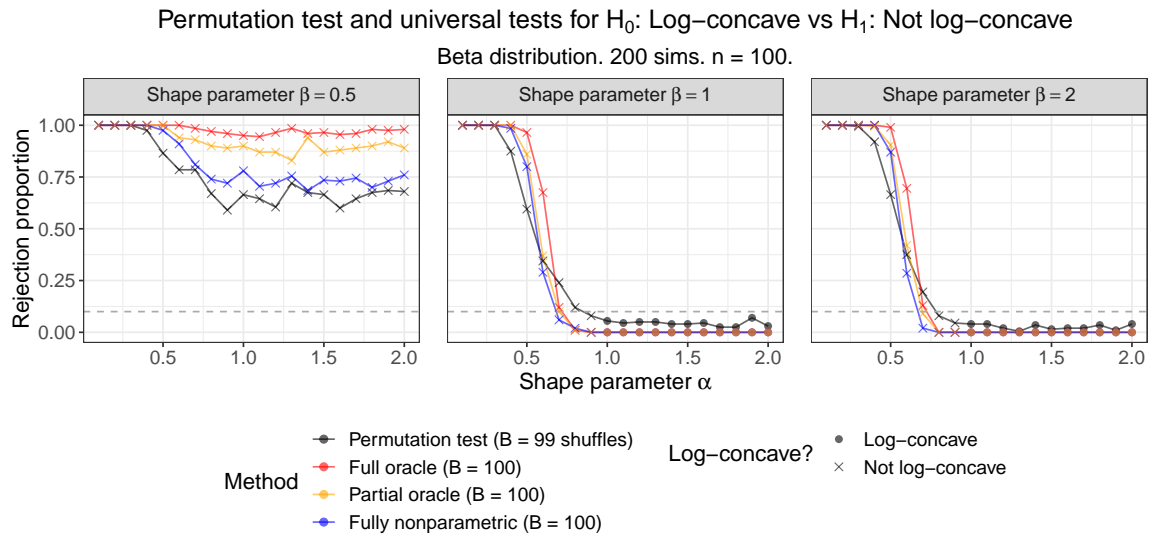


Figure 17: Rejection proportions for four tests of $H_0 : f^*$ is log-concave versus $H_1 : f^*$ is not log-concave, on $\text{Beta}(\alpha, \beta)$ density. The permutation test is valid in all simulations, but the universal tests have both higher power and guaranteed validity.